

HIERARCHICAL TRANSFORMER WITH SPATIO-TEMPORAL CONTEXT AGGREGATION FOR NEXT POINT-OF-INTEREST RECOMMENDATION

Jiayi Xie¹ and Zhenzhong Chen^{1,*}

¹School of Remote Sensing and Information Engineering, Wuhan University

ABSTRACT

Next point-of-interest (POI) recommendation is a critical task in location-based social networks, yet remains challenging due to a high degree of variation and personalization exhibited in user movements. In this work, we explore the latent hierarchical structure composed of multi-granularity short-term structural patterns in user check-in sequences. We propose a Spatio-Temporal context AggRegated Hierarchical Transformer (STAR-HiT) for next POI recommendation, which employs stacked hierarchical encoders to recursively encode the spatio-temporal context and explicitly locate subsequences of different granularities. More specifically, in each encoder, the global attention layer captures the spatio-temporal context of the sequence, while the local attention layer performed within each subsequence enhances subsequence modeling using the local context. The sequence partition layer infers positions and lengths of subsequences from the global context adaptively, such that semantics in subsequences can be well preserved. Finally, the subsequence aggregation layer fuses representations within each subsequence to form the corresponding subsequence representation, thereby generating a new sequence of higher-level granularity. The stacking of encoders captures the latent hierarchical structure of the check-in sequence, which is used to predict the next visiting POI. Extensive experiments on three public datasets demonstrate that the proposed model achieves superior performance whilst providing explanations for recommendations. Codes are available at <https://github.com/JennyXieJiayi/STAR-HiT>.

1 INTRODUCTION

With the prevalence of location-based services provided by applications such as Foursquare, Uber, Facebook, users are getting used to sharing their location-based experiences and acquiring location-aware services online. One of the most common location-based services is Point-of-Interest (POI) recommendation, which aims to predict the POI that is most likely to be visited by users. Next POI recommendation is a sub-field of POI recommendation that focuses on exploiting the user's historical trajectory to discover the potential sequential behavior patterns. On the one hand, next POI recommendation satisfies the personalized needs of users and alleviates information overload. On the other hand, it helps location-based service providers to provide intelligent location services, such as location-aware advertising, real-time Q&A revolving around POIs, *etc.* Therefore, next POI recommendation plays an increasingly important role in location-based services, and has attracted lots of attention from researchers in both academia and industry.

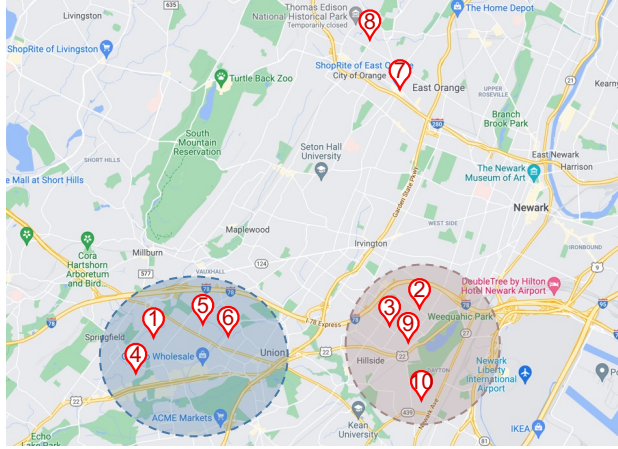
Next POI recommendation has been extensively studied [1, 2]. Early studies focus on feature engineering (*e.g.*, geospatial, temporal, social, content feature) and conventional machine learning models, such as Markov Chain (MC) based stochastic models and Matrix Factorization (MF) models to capture POI-POI transitions [3, 4]. These models rely on a strong assumption that the next POI for users to check-in is only determined by the last one or several check-ins. However, the next POI visited by a user is also highly correlated to other previous check-ins. As deep learning methods have shown promising performance

compared to conventional methods, recent work turned to utilizing deep learning approaches to boost the performance of next POI recommendation [5, 6]. Among them, many studies adopt Recurrent Neural Network (RNN) to mine more complicated sequential patterns in long-term semantics [6, 7, 8]. They extend RNNs with the ability to effectively incorporate various contextual information, especially the spatio-temporal context. Some work also takes advantage of other deep learning techniques, such as attention mechanisms [9, 10], memory networks [11], pre-training models [12], meta-learning paradigms [13], *etc.*

Most previous methods assume that users only have preferences for some specific POIs, ignoring short-term structural patterns exhibited in user movements [14]. Such short-term structural patterns are highly personalized that can be caused by temporal regularities and geospatial constraints, resulting in multiple semantic subsequences at multi-level that comprise consecutive check-ins. The next visiting POI of the user could be correlated to several subsequences, which represent preferences beyond POI-level. As a special case shown in Figure 1, a user often visits the area near her workplace (*i.e.*, POI 2, 3) because of the convenience of visiting, instead of preferring a specific restaurant. Thus, other restaurants in that area could be the potential POI she would like to visit (*i.e.*, POI 9). Such a high-level pattern can be inferred if she periodically visits the workplace area. Furthermore, the short-term sequential patterns could be multiple granularities. In particular, the user visits POIs in the home-workplace area in a regular manner (except POI 7, 8), such that the combination of check-in subsequences in the home area and workplace area could constitute the subsequence of a higher level granularity.

In order to exploit the aforementioned hierarchical structure of the check-in sequence, a naive way is to use a fixed-length subsequence embedding under an implicit assumption that the

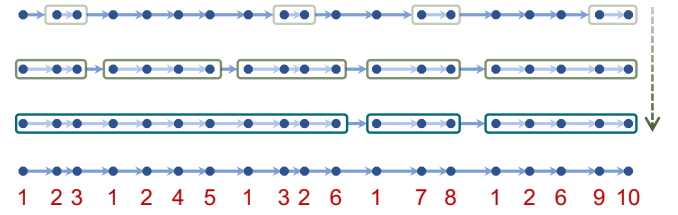
* Corresponding author.



(a) Map



(b) Check-in Sequence



(c) Subsequence Aggregation

Figure 1: A check-in sequence example.

fixed-length subsequence is suitable for all short-term structural patterns in the check-in sequence. Such hard sequence partition neglects the personalized sequential behavior and could damage the semantic information. Nevertheless, it is challenging to identify and integrate multi-level semantic subsequences due to the difficulty of pre-defining granularities and lengths of subsequences [8]. How to comprehensively understand the overall sequential behavior patterns of users by discovering multi-level semantic subsequences remains to be explored.

In light of the above, in this work, we aim to explore the latent hierarchical structure of the user movement by adaptively locating the semantic subsequence of multiple granularities in the check-in sequence. We propose a Spatio-Temporal context AggRegated Hierarchical Transformer (STAR-HiT) for next POI recommendation, which employs a stack of hierarchical encoders to jointly model the spatio-temporal context and capture the latent hierarchical structure in the check-in sequence. In particular, we design and stack the hierarchical encoder to recursively encode the spatio-temporal context and explicitly locate semantic subsequences, and generate subsequence representations to form a new sequence with a higher level of granularity. Note that every single check-in in the original check-in sequence can be regarded as the shortest subsequence. In each encoder, the global attention layer is utilized to capture the spatio-temporal correlations between subsequences, such that subsequences with similar sequential patterns could be associated. After the global context modeling, the sequence partition layer learns to adaptively locate next-level subsequences, followed by a local attention layer performed within each identified subsequence to enhance subsequence modeling using the corresponding local context. Finally, the subsequence aggregation layer fuses the representations in each next-level subsequence individually to form the subsequence representation, thereby generating a new sequence with a higher level of granularity. This sequence is then fed into the next encoder for further subsequence integrating and sequence abstraction. The intermediate representations in each encoder are learned to be expressive about the spatio-temporal context based on the global and local attention mechanisms; meanwhile, the sequence partition and subsequence aggregation

operation can flexibly discover semantic subsequences of different positions and lengths. To summarize, this work makes the following main contributions:

1. A novel next POI recommendation model STAR-HiT, consisting of stacked hierarchical encoders, is proposed to capture the latent hierarchical structure of the check-in sequence, from which the personalized movement pattern is revealed for the recommendation.
2. A hierarchical encoder is designed to encode the spatio-temporal context and adaptively identify subsequences with different positions and lengths in the input sequence, then generate a sequence with a higher level of granularity. By stacking multiple hierarchical encoders, semantic subsequences of different granularities are recursively identified and integrated, so as to expose the overall hierarchical structure presented in the user movement.
3. By capturing multi-level semantic subsequences that uncover the hierarchical structure, STAR-HiT guarantees the robustness and explainability of recommendations. Extensive experiments conducted on three public datasets demonstrate that our proposed STAR-HiT outperforms state-of-the-art models by a large margin whilst providing explanations for recommendations.

The remaining of this paper is organized as follows: in Section 2, we review the related work. Section 3 expounds on the proposed STAR-HiT in detail, followed by experimental results with analysis on three public datasets in Section 4. Finally, Section 5 concludes the work.

2 RELATED WORK

In this section, we first review the related work in the field of sequential recommendation and next POI recommendation. Then, we take a brief look at hierarchical Transformers applied to Natural Language Processing (NLP) and Computer Vision (CV).

2.1 Sequential Recommendation

Sequential recommendation mines behavior patterns in user action (e.g., click, watch, comment) sequences. Early work usually models an item-item transition pattern based on Markov chains. For example, Rendle *et al.* [15] proposed the Factorized Personalized Markov Chains (FPMC) model that combines matrix factorization and Markov chains to incorporate both general preference and sequential behavior. Some studies follow this work and extend it to higher-order Markov chains [16, 17], where an L -order Markov chain is utilized to make predictions based on the L previous actions. In general, Markov chain based models mainly focus on the latest short-term preference, performing relatively well in high-sparsity scenarios. With recent advances in deep learning, lots of work adopts neural network architectures, such as Convolutional Neural Networks (CNNs) [18, 19], Recurrent Neural Networks (RNNs) [20, 21], Graph Neural Networks (GNNs) [22, 23], *etc.* Among them, RNN is the most commonly used backbone, which encodes long-term dependencies in variable-length sequences. It performs well on dense datasets while exhibiting relatively poor performance on sparse datasets. Furthermore, some advanced deep learning techniques are utilized to enhance modeling capabilities, such as attention mechanisms [24], memory networks [25], data augmentation [26], denoising [27] and pre-training techniques [28], *etc.* More recently, Transformer-based approaches have shown remarkable performance in sequential recommendation. For instance, Kang *et al.* [29] proposed a Self-Attention based Sequential Recommendation model (SASRec) that directly utilizes the stacked self-attention blocks in the vanilla Transformer to capture the correlation between every two items in the action sequence. SASRec outperforms state-of-the-art MC/CNN/RNN-based sequential recommendation methods on both sparse and dense datasets. Sun *et al.* [30] employed deep bidirectional self-attention to better model user behavior sequences. Later on, Li *et al.* [31] improved SASRec by explicitly modeling the timestamps of interactions to emphasize the temporal influence. Wu *et al.* [32] introduced the personalization into SASRec by learning user embeddings with stochastic shared embeddings regularization. Moreover, Liu *et al.* [33] alleviated the cold-start issue by augmenting short sequences with a pre-trained Transformer, which is trained on the reversed behavior sequences.

2.2 Next POI Recommendation

Next POI recommendation can be regarded as a special case of sequential recommendation, where geospatial influence is one of the most crucial context to be involved. Similar to the research on sequential recommendation, early studies on next POI recommendation mainly utilize Markov chains and matrix factorization [3, 4, 34]. Cheng *et al.* [3] extended FPMC model to FPMC-LR that models the personalized POI transition while considering users' movement constraint, namely, moving around a localized region. Feng *et al.* [4] further replaced the matrix factorization method with a metric embedding method and exploited the pair-wise ranking scheme to learn parameters. He *et al.* [34] adopted a third-rank tensor to model the successive check-in behaviors and incorporated the softmax function to fuse the personalized Markov chain with users' latent behavior patterns.

With the surge of deep learning research, a large variety of next

POI recommendation approaches leveraging different deep learning paradigms have been proposed. Among them, some work employs the word2vec framework [5] to learn representations of POIs, which can reflect the contextual relationships of several continuously visited POIs [35, 36]. In addition, most existing models are based on RNNs, which have been widely applied to sequential data due to their powerful capability to exhibit temporal dynamics. For example, Liu *et al.* [6] adopted RNN to model the user's check-in sequence. The proposed ST-RNN model captures the spatial and temporal context with the time and distance transition matrices. Yang *et al.* [37] jointly modeled social networks and mobile trajectories by deriving user representations from social networks and adopting two different RNNs to encode long- and short-term sequential influence. Feng *et al.* [38] enhanced GRU by utilizing attention mechanisms that capture the multi-level periodicity of users' mobility from long-range and sparse trajectories. Moreover, Guo *et al.* [39] employed LSTM as the recurrent layer, and designed a meta-path based random walk over a knowledge graph to discover location neighbors based on heterogeneous factors. Zhao *et al.* [7] extended the LSTM gating mechanism with the spatial and temporal gates to capture the user's space and time preference. Zhao *et al.* [8] introduced a binary boundary detector into RNN and modified the gating mechanism to learn the sequential patterns of semantic subsequences in the check-in sequence, then utilized a power-law attention mechanism to integrate the spatio-temporal context. Sun *et al.* [40] combined a non-local network and a geo-dilated LSTM to leverage both long-term preference and geographical influence. Zang *et al.* [41] explored the category hierarchy of POIs to develop an attention-based knowledge graph for POI representation learning, and then proposed a spatial-temporal decay LSTM to capture the personalized behavior pattern. The above RNN-based models present many novel and enlightening contributions for introducing spatio-temporal context modeling into neural networks. Nevertheless, as aforementioned, RNN-based models need relatively dense data to train, while data sparsity is one of the most crucial problems in practical scenarios [2].

Similar to sequential recommendation, some work also takes advantage of other deep learning techniques, such as attention mechanisms [10, 9], memory networks [11], pre-training strategies [12], meta-learning paradigms [13, 42], *etc.* In particular, Zhou *et al.* [11] proposed a Topic-Enhanced Memory Network that combines the topic model and memory network to jointly capture the global structure of latent patterns and local neighborhood-based features, while incorporating geographical influence by calculating a comprehensive geographical score. Kim *et al.* [13] proposed an adaptive weighting scheme based on meta-learning to alleviate the class imbalance problem and noise of the input data. Cui *et al.* [42] jointly utilized a sequential knowledge graph and a meta-learning strategy to learn and optimize latent embeddings, thus modeling user check-in patterns while alleviating the data sparsity issue. As for attention-based models, Luo *et al.* [10] employed a bi-layer attention architecture that allows global point-point interaction within the trajectory. The proposed method explicitly models the spatio-temporal context by embedding the spatio-temporal relation matrix of the trajectory. Lian *et al.* [9] developed a self-attention model to encode the check-in sequence, and encoded the hierarchical gridding of geospatial information with another self-attention

based encoder. Lin *et al.* [12] built a pre-training model to adaptively generate embeddings for locations based on their specific contextual neighbors.

Although some studies have been devoted to investigating the short-term periodicity in the check-in sequence to optimize the network architecture [38, 39, 8, 41], most previous work neglected the complicated yet structural patterns exhibited in user movements. In this work, we adopt the Transformer structure that has shown the convincing capability of dealing with long-term dependencies in sequences, and capture the latent hierarchical structure of user movements by adaptively discovering the multi-level semantic subsequences in an explicit way.

2.3 Hierarchical Transformers

Transformer architectures are based on the self-attention mechanism that learns the relationships among every element of a sequence, which can attend to complete sequences, thereby comprehensively understanding long-term context. Transformer was first proposed by Vaswani *et al.* [43] for machine translation, and has since become the state-of-the-art method in many NLP tasks. There are two mainstream approaches to enhancing the Transformer for better modeling longer-range dependencies with higher efficiency: variant self-attention mechanisms [44, 45] and hierarchical Transformer structures [46, 47, 48, 49]. Here we focus on the latter that leverages the natural hierarchical structure present in the syntax. Liu *et al.* [46] developed a multi-document summarization model and adopted a local Transformer layer and a global Transformer layer to encode the intra- and inter-paragraph contextual information, respectively. Yang *et al.* [48] proposed a Siamese Multi-depth Transformer for document representation learning and matching, which contains sentence blocks and document context modeling. Wu *et al.* [49] effectively modeled long documents by a hierarchical Transformer following the sentence-document-sentence encoding strategy such that both sentence level and document level context could be integrated.

The breakthroughs of Transformers in NLP have sparked great interest in CV tasks. Transformers for vision tasks usually segment the input image into a sequence of patches and capture long-range dependencies among patches. For example, Dosovitskiy *et al.* [50] introduced the Vision Transformer for image classification, the first work directly applying the Transformer architecture and dispensing with convolutions entirely. To fit the Transformer, the input image is split into fix-size patches and linearly embedded into flat tokens to construct the input sequence. Liu *et al.* [51] extended Vision Transformer by shifted windows, improving the efficiency by limiting the self-attention computation solely within each local window. They constructed hierarchical representations that start from small-sized patches and gradually merged neighboring patches in deeper layers. Wang *et al.* [52] improved Vision Transformer by incorporating the pyramid structure from convolutional neural networks. They utilized fine-to-coarse image patches to reduce the sequence length of Transformer as the network deepens, such that the input sequence elements can be set to pixel-level for dense prediction without increasing computational cost. Later on, Chen *et al.* [53] drew on the deformable convolution [54] and replaced the pre-defined patches with learnable patches in a data-driven way. As the proposed deformable patch embedding module

splits the image into patches in a deformable way with learnable patch size and location, the semantics in patches can be well preserved.

Our work is partially inspired by the hierarchical enhancement of Transformer structures. In spite of the outstanding performance that these hierarchical Transformers have shown in various tasks, they cannot be directly used for next POI recommendation. Unlike the syntactic knowledge that helps pre-define the multi-scale subsequences for language modeling, the subsequences in the check-in sequence are personalized; thus, the extraction by a fixed length is unsuitable. Besides, the grid-topology spatial structure of visual data distinguishes them from check-in sequences, leading to the incompatibility of visual hierarchical Transformers to next POI recommendation. Nevertheless, these pioneering studies motivate us to extend Transformers to adaptively learn semantic multi-grained subsequences in the check-in sequence for better sequential behavior understanding.

3 METHODOLOGY

In this section, we first formulate the next POI recommendation task, then elaborate on the details of the proposed Spatio-Temporal context AggRegated Hierarchical Transformer (STAR-HiT). The notations mainly used in this article are listed in Table 1.

3.1 Problem Statement

Let $\mathcal{U} = \{u_1, u_2, \dots, u_m\}$, $\mathcal{P} = \{p_1, p_2, \dots, p_n\}$ be the set of users and POIs, respectively. $\mathcal{S} = \{S_1, S_2, \dots, S_m\}$ represents the set of user check-in sequences. For each user u , her check-in trajectory in chronological order is denoted as $S_u = \{s_t^{(u)} \mid t = 1, 2, \dots, L\}$, where $s_t^{(u)} = (p_t, g_t, \tau_t)$ is the t -th check-in that user u visits POI $p_t \in \mathcal{P}$ with the geographic location $g_t = (\text{latitude} = \alpha_t, \text{longitude} = \beta_t)$ at timestamp τ_t .

Next POI recommendation aims to recommend the POI that is most likely to be visited by the user at the next time step. Given a user u with her check-in sequence S_u , the goal is to predict the next visiting POI $p_{t+1} \in \mathcal{P}$. The task can be formulated as estimating the personalized ranking score to the POI by:

$$\hat{y}_{u,p} = f_{\Theta}(p \in \mathcal{P} \mid u, S_u), \quad (1)$$

where $f_{\Theta}(\cdot)$ denotes the underlying model with parameters Θ , and $\hat{y}_{u,p}$ is the predicted score for the check-in that user u would like to visit POI p at next time step. The top- k POIs ranked by predicted scores are the final recommendations.

3.2 Overall Architecture

As shown in Figure 2, our proposed STAR-HiT consists of an embedding module, stacked hierarchical encoders, and the predictor. In particular, the embedding module embeds the POI and spatio-temporal context into latent representations to construct the spatio-temporal aware representation matrix of the check-in sequence. As for the stacked hierarchical encoders, the encoder adopts a hierarchical architecture that abstracts the input sequence to a compressive and expressive sequence. More specifically, the encoder first models the global spatio-temporal

Table 1: Notations Used in This Article

Variables	Description
m, n, L	the number of users, POIs, and the length of the check-in sequence
d, d_h, d_k	dimensions of latent representations
u, \mathcal{U}	a user and the user set
p, \mathcal{P}	a POI and the POI set
S_u, \mathcal{S}	the check-in sequence of the user u , the check-in sequence set
$s_t^{(u)}$	the t -th check-in of the user u
g, τ	geographic location and timestamp
$\Delta^S \in \mathbb{R}^{L \times L}$	spatial relation matrix
$\Delta^T \in \mathbb{R}^{L \times L}$	temporal relation matrix
k	the initial length of the subsequence
l	the number of stacked hierarchical encoders
$\mathbf{E}(u) \in \mathbb{R}^{L \times d}$	the representation matrix of the check-in sequence S_u
$\mathbf{E}(u)^{(l)} \in \mathbb{R}^{\lceil \frac{L}{k} \rceil \times d}$	the representation matrix after l hierarchical encoders of the check-in sequence S_u

context within the entire sequence, or in other words, models the relationships between different subsequences learned in the previous encoder. Note that every single check-in in the very beginning check-in sequence is viewed as the shortest subsequence. Then the sequence is adaptively partitioned into next-level semantic subsequences with learnable positions and lengths, followed by the local context enhancement. Next-level subsequence representations are obtained by fusing their containing representations, which form the output sequence with a higher level of granularity. The hierarchical structure of the check-in sequence composed of multi-level semantic subsequences is learned based on stacked hierarchical encoders, with the purpose of comprehensively understanding users' overall sequential behavior patterns. Finally, a Multi-Layer Perceptron (MLP) based predictor is exploited to predict the check-in probabilities for users visiting POI. The details of STAR-HiT are elaborated as follows.

3.3 Embedding Module

The embedding module consists of two parts: a trajectory embedding layer and a spatio-temporal context embedding layer.

3.3.1 Trajectory embedding layer

The trajectory embedding layer encodes check-in POIs into latent representations of dimension d . We use $e^{p_t} \in \mathbb{R}^d$ to denote the embedding of POI p_t for user's t -th visiting. The embedding of each check-in sequence S_u is represented as $\hat{\mathbf{E}}(u) = [e^{p_1}; e^{p_2}; \dots; e^{p_L}] \in \mathbb{R}^{L \times d}$, where L is the length of the sequence. The user embedding like [9, 10] adopted is discarded, as the personalized information is already well preserved in the spatio-temporal context embedding to be introduced next.

3.3.2 Spatio-temporal context embedding layer

To leverage the spatio-temporal context of the check-in sequence, we first calculate the time intervals and geographical distances between every two visited POIs in a trajectory to construct the spatial-temporal relation matrices.

Following [9], for each check-in sequence S_u , we used $\Delta_{i,j}^S = \text{Haversine}(p_i, p_j)$ to obtain the distance between i -th and j -th visiting POI given their longitudes and latitudes¹. As for time intervals, instead of directly calculating the timestamp differences or uniformly grouping the values into discrete bins as [6, 10] did, we resort to the scale of time intervals. Due to the extremely high variance of time intervals (*e.g.*, from a few minutes to several years), we group the time interval into M levels, namely, $\Delta_{i,j}^T \in [1, M]$, $M \in \mathbb{N}$, indicating the scale of the time interval between two check-ins ranging from within an hour to over a year. M is set to 7 in our implementation.

According to Tobler's First Law of Geography [55, 56], near POIs are more related than distant ones, which exhibits strong geographical influence. Inspired by [57, 8], we can consider that the probability of visiting a pair of POIs p_i and p_j for user u follows the power-law distribution as:

$$\Pr(p_i, p_j) = a \cdot D(p_i, p_j)^{-\lambda}, \quad (2)$$

where a and λ are learnable parameters of the power-law distribution, $D(p_i, p_j)$ is the distance between POI p_i and p_j . We take the logarithm on both sides of Equation (2) as:

$$\log(\Pr(p_i, p_j)) = \log(a) + \lambda \cdot \log(D(p_i, p_j)). \quad (3)$$

By leveraging the temporal influence, we extend Equation (3) by replacing the learnable $\log(a)$ with the temporal context as:

$$\log(\Pr(p_i, p_j)) = T(p_i, p_j) + \lambda \cdot \log(D(p_i, p_j)), \quad (4)$$

where $T(p_i, p_j)$ represents the time interval between visiting p_i and p_j . As such, both geographical and temporal influences are incorporated into the calculation of co-visiting probability. Furthermore, λ can be regarded as controlling the trade-off between geographical and temporal influence.

With the spatial relation matrix Δ^S and temporal relation matrix Δ^T , we can obtain the spatio-temporal context embedding matrix $\mathbf{E}_c(u)$ of the check-in sequence S_u as:

$$\mathbf{E}_c(u) = \Delta^T + \lambda \cdot \log(\Delta^S). \quad (5)$$

¹Haversine formula calculates the great-circle distance between two points on a sphere given their longitudes and latitudes.

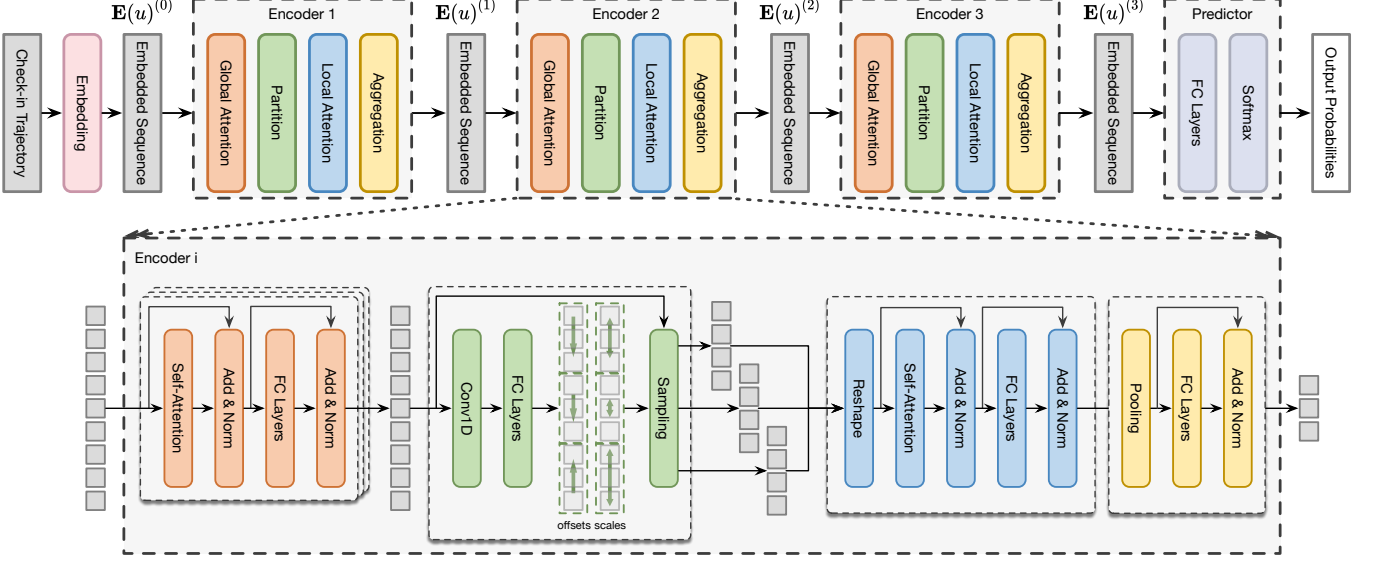


Figure 2: The framework of the proposed STAR-HiT model.

We fuse all contextual information by concatenating the trajectory embedding and spatio-temporal context embedding, and then apply a linear transformation with learnable weights $\mathbf{W}^E \in \mathbb{R}^{(L+d) \times d}$ to obtain the final embedding of the check-in sequence:

$$\mathbf{E}(u) = \text{Concat}([\hat{\mathbf{E}}(u); \mathbf{E}_c(u)])\mathbf{W}^E. \quad (6)$$

Since the self-attention mechanism contains no recurrence and no convolution to capture relative positions in the sequence like RNN, we follow [43] to add positional encodings \mathbf{P} into $\mathbf{E}(u)$, i.e., $\mathbf{E}(u) = \mathbf{E}(u) + \mathbf{P}$.

3.4 Hierarchical Encoder

In order to capture semantic subsequences of multiple granularities to obtain the hierarchical structure of the check-in sequence, the hierarchical encoder is supposed to extract semantic subsequences in the input sequence and derive their representations to generate a shorter output sequence with higher-level representations of behavior patterns. To this end, the proposed encoder comprises: 1) **global attention layer** that models the global context, 2) **sequence partition layer** that learns to locate semantic subsequences with different positions and lengths, 3) **local attention layer** that enhances subsequence modeling using the local context, 4) **subsequence aggregation layer** that obtains subsequence representations to construct a new sequence with an increased abstraction level. The details of the hierarchical encoder are shown at the bottom of Figure 2.

3.4.1 Global Attention

The global attention layer aims to learn the global context in the input sequence. Here, we adopt the encoder layer in the vanilla Transformer that contains two sub-layers, i.e., the multi-head self-attention sub-layer and position-wise feed-forward sub-layer. To briefly revisit Transformer, each encoder layer adaptively aggregates the values according to the attention weights

that measure the compatibility of query-key pairs, where the query, key, value are all vectors transformed from the input representation. Such point-point interaction within the sequence allows the layer to capture long-term dependencies. Moreover, multi-head self-attention enables the layer to jointly attend to information from different representation subspaces at different positions.

In our case, the multi-head self-attention operation takes the embedding $\mathbf{E}(u)$ as input, linearly projects it into h subspaces through distinct matrices, and then applies h attention functions in parallel to produce the output representations, which are concatenated and once again projected. The whole multi-head self-attention operation can be summarized as follows:

$$\text{MSA}(\mathbf{E}(u)) = \text{Concat}([\mathbf{SA}_1, \mathbf{SA}_2, \dots, \mathbf{SA}_h])\mathbf{W}^O, \quad (7)$$

where

$$\mathbf{SA}_i = \text{Attention}(\mathbf{E}(u)\mathbf{W}_i^Q, \mathbf{E}(u)\mathbf{W}_i^K, \mathbf{E}(u)\mathbf{W}_i^V). \quad (8)$$

The projection matrices for each head $\mathbf{W}_i^Q \in \mathbb{R}^{d \times d_h}$, $\mathbf{W}_i^K \in \mathbb{R}^{d \times d_h}$, $\mathbf{W}_i^V \in \mathbb{R}^{d \times d_h}$, $\mathbf{W}^O \in \mathbb{R}^{d \times d}$ are learnable parameters, where $d_h = d/h$. Note that the superscript (l) indicating the l -th encoder is omitted above for simplicity. Here, the attention function is scaled dot-product attention, which is calculated as follows:

$$\text{Attention}(\mathbf{Q}, \mathbf{K}, \mathbf{V}) = \text{softmax}\left(\frac{\mathbf{Q}\mathbf{K}^T}{\sqrt{d_h}}\right)\mathbf{V}. \quad (9)$$

The multi-head self-attention sub-layer is followed by a position-wise feed-forward sub-layer, a fully connected two-layer feed-forward network applied to each position separately and identically. This consists of two linear transformations with a ReLU activation in between:

$$\text{FFN}(x) = \text{ReLU}(0, x\mathbf{W}_1 + \mathbf{b}_1)\mathbf{W}_2 + \mathbf{b}_2, \quad (10)$$

where $\mathbf{W}_1 \in \mathbb{R}^{d \times d_k}$, $\mathbf{W}_2 \in \mathbb{R}^{d_k \times d}$ and $\mathbf{b}_1 \in \mathbb{R}^{d_k}$, $\mathbf{b}_2 \in \mathbb{R}^d$, s.t. $d_k > d$ are learnable parameters and shared across all positions. In addition, we also adopt residual connection [58], layer normalization [59], and dropout regularization [60] to refine the network

structure [43, 30]. More specifically, we employ the residual connection around each of the two sub-layers, followed by layer normalization. The dropout is applied to the output of each sub-layer, before it is normalized. In summary, the sequence representation matrix after encoding the global context via the global attention layer is formulated as follows:

$$\begin{aligned}\hat{\mathbf{E}}_G(u) &= \text{LayerNorm}(\mathbf{E}(u) + \text{Dropout}(\text{MSA}(\mathbf{E}(u)))), \\ \mathbf{E}_G(u) &= \text{LayerNorm}(\hat{\mathbf{E}}_G(u) + \text{Dropout}(\text{FFN}(\hat{\mathbf{E}}_G(u)))).\end{aligned}\quad (11)$$

3.4.2 Sequence Partition

In order to extract semantic subsequences in the check-in sequence, we first divide the sequence uniformly into $\lceil \frac{L}{k} \rceil$ non-overlapping subsequences of length k . Let x_i denote the center coordinate of the i -th subsequence in the check-in sequence S_u , such that the location range of the subsequence in the input sequence is initialized as $(x_i - k/2, x_i + k/2)$. Next, we set the center coordinate x_i and the length k_i of each subsequence into learnable parameters, which can be inferred from the spatio-temporal context. In particular, inspired by [53] for semantic patch learning in vision tasks, we predict the offset dx_i and length k_i based on the sequence representation $\mathbf{E}_G(u)$ as follows:

$$\begin{aligned}dx_i &= \text{Tanh}(w^1 \cdot f(\mathbf{E}_G(u)_i)), \\ k_i &= \text{ReLU}(\text{Tanh}(w^2 \cdot f(\mathbf{E}_G(u)_i))),\end{aligned}\quad (12)$$

where hyper-parameters w^1, w^2 control the weights of the offset and length to update the subsequence location, and $\mathbf{E}_G(u)_i$ is the representation matrix slicing corresponding to the i -th subsequence. $f(\cdot)$ denotes the feature extractor that learns the offset and length from subsequence representations. We follow [53] and implement the feature extractor as a 1D convolution and a linear transformation with a ReLU activation in between.

Accordingly, the i -th learned subsequence is located in $(x_i + dx_i - k_i/2, x_i + dx_i + k_i/2)$. In this way, we can fully exploit the context to discover semantic subsequences. However, the subsequence with variable length makes it impractical to encode the intra-subsequence context subsequently. As a result, we introduce the sampling strategy to derive fixed-length subsequences. Given the location range of a subsequence in the input sequence $(x_{\text{left}}, x_{\text{right}})$, we first linearly interpolate r points as (x_1, x_2, \dots, x_r) inside the subsequence. As the interpolated coordinates could be fractional, we then use the nearest-neighbor sampling to take representations closest to the corresponding coordinates, denoting as $\{\hat{e}^{[x_j]} \mid j = 1, 2, \dots, r\}$. Here we omit the superscript (i) indicating the index of the subsequence for clarity. Finally, we concatenate the sampling representations as:

$$\mathbf{E}_P(u)_i = \text{Concat}([\hat{e}^{[x_1]}; \hat{e}^{[x_2]}; \dots; \hat{e}^{[x_r]}]), \quad (13)$$

so as to obtain the representation matrix of the i -th subsequence $\mathbf{E}_P(u)_i \in \mathbb{R}^{r \times d}$. In our implementation, the number of samples r for each subsequence is set to the same as the initial length k of subsequences.

3.4.3 Local Attention

As semantic subsequences are identified, a local attention layer is applied afterward for encoding local contextual information

within each subsequence. We use the same attention function as in Equation (9) with only one head, since the subsequences are much shorter. We stack the current subsequence representations as $\mathbf{E}_P(u) \in \mathbb{R}^{\lceil \frac{L}{k} \rceil \times r \times d}$, such that the attention function for all subsequences can be computed in parallel as follows:

$$\text{SA}_L(\mathbf{E}_P(u)) = \text{Attention}(\mathbf{E}_P(u)\mathbf{W}_L^Q, \mathbf{E}_P(u)\mathbf{W}_L^K, \mathbf{E}_P(u)\mathbf{W}_L^V)\mathbf{W}_L^O, \quad (14)$$

where

$$\text{Attention}(\mathbf{Q}, \mathbf{K}, \mathbf{V}) = \text{softmax}\left(\frac{\mathbf{Q}\mathbf{K}^T}{\sqrt{d}}\right)\mathbf{V}. \quad (15)$$

The projection matrices $\mathbf{W}_L^Q \in \mathbb{R}^{d \times d}$, $\mathbf{W}_L^K \in \mathbb{R}^{d \times d}$, $\mathbf{W}_L^V \in \mathbb{R}^{d \times d}$ and $\mathbf{W}_L^O \in \mathbb{R}^{d \times d}$ are learnable parameters, where $\mathbf{W}_L^Q, \mathbf{W}_L^K, \mathbf{W}_L^V$ are shared across all subsequence representation matrices. Except for the local attention function calculated within each subsequence, the rest of the local attention layer is the same as the global attention layer, with individual parameters. Ultimately, the whole local attention layer can be described as follows:

$$\begin{aligned}\hat{\mathbf{E}}_L(u) &= \text{LayerNorm}(\mathbf{E}_P(u) + \text{Dropout}(\text{SA}_L(\mathbf{E}_P(u)))), \\ \mathbf{E}_L(u) &= \text{LayerNorm}(\hat{\mathbf{E}}_L(u) + \text{Dropout}(\text{FFN}(\hat{\mathbf{E}}_L(u)))).\end{aligned}\quad (16)$$

3.4.4 Subsequence Aggregation

After context modeling via attention mechanisms and sequence partitioning into semantic subsequences, we gather the representations within each subsequence to obtain the corresponding subsequence representations, which constitute the output sequence.

Given the representation matrix $\mathbf{E}_L(u)$, the representation of the i -th subsequence is obtained by the average pooling of the representations of all representations it contains, which is formulated as:

$$\hat{\mathbf{E}}_A(u)_i = \frac{1}{r} \sum_{j=ir}^{(i+1)r} \mathbf{E}_L(u)_{i,j}, \quad (17)$$

followed by a fully connected two-layer feed-forward network as in Equation (10), with the aforementioned techniques that ease the training. Accordingly, the output of the subsequence aggregation layer, as well as the output of the hierarchical encoder, is obtained by:

$$\mathbf{E}_A(u) = \text{LayerNorm}(\hat{\mathbf{E}}_A(u) + \text{Dropout}(\text{FFN}(\hat{\mathbf{E}}_A(u)))). \quad (18)$$

By now, the structure of the proposed hierarchical encoder is fully specified. Through the hierarchical encoder, the global context of the sequence and local contexts of semantic subsequences are well involved, while the input sequence $\mathbf{E}(u)^{(l-1)} \in \mathbb{R}^{\lceil \frac{L}{k^{(l-1)}} \rceil \times d}$ of the l -th encoder are abstracted to the output sequence $\mathbf{E}(u)^{(l)} = \mathbf{E}_A(u)^{(l)} \in \mathbb{R}^{\lceil \frac{L}{k^{(l)}} \rceil \times d}$, where (l) indicates the l -th encoder. Besides, semantics subsequences in each encoder are identified by the learned positions and lengths.

3.4.5 Stacking Encoders

In order to model the latent hierarchical structure of the sequential behavior pattern from the check-in sequence, we stack the hierarchical encoders to recursively partition the input sequence

into multiple semantic subsequences and aggregate them to form the output sequence with different levels of granularity.

As aforementioned, the length of sequence is reduced from L to $\lceil \frac{L}{k} \rceil$ after l hierarchical encoders. The output of the hierarchical encoder stack would be of shorter length while highly informative about the personalized behavior sequential pattern; meanwhile, each encoder is learned to be capable of discovering semantic subsequences with different levels of granularity. The number of stacked encoders l will be discussed in Section 4.3.1.

3.5 Prediction

To predict the next check-in POI, we first obtain the user representation U_u of user u by summing up the output $E(u)^{(l)}$ after the stack of l hierarchical encoders, which constitutes the user representation matrix $U \in \mathbb{R}^{m \times d}$ that represents the personalized sequential behavior patterns of all users.

A commonly used prediction layer adopted the matching function as follows:

$$\hat{y}_{u,p} = U_u^\top P_p, \quad (19)$$

where P_p is the embedding of POI $p \in \mathcal{P}$ [29, 10]. However, further adding the POI embeddings to calculate the matching score degrades the performance of the proposed STAR-HiT to some extent. The main reason may lie in the difference between the personalized representation encoded by encoders and the general representation obtained by the embedding layer. Therefore, the matching function is not adopted in our implementation. Instead, we directly use a linear transformation with learnable weight $W^P \in \mathbb{R}^{d \times n}$ and a softmax function to convert the output into predicted next POI probabilities as follows:

$$\hat{y}_u = \text{softmax}(U_u W^P), \quad (20)$$

where $\hat{y}_u = [\hat{y}_{u,1}, \hat{y}_{u,2}, \dots, \hat{y}_{u,n}]$ is the predicted score of user u to visit the candidate POIs.

To train the model, we adopt the cross-entropy loss to optimize parameters as:

$$\mathcal{L} = - \sum_{S_u \in \mathcal{S}_{\text{training}}} (\log \hat{y}_{u,i} + \sum_{j \in \mathcal{P}, j \neq i} \log(1 - \hat{y}_{u,j})), \quad (21)$$

where $\mathcal{S}_{\text{training}}$ is the training set of check-in sequences.

4 EXPERIMENTS

In this section, we conduct experiments to show the effectiveness of the proposed STAR-HiT. Specifically, we aim to answer the following research questions:

- **RQ1:** How does STAR-HiT perform compared to state-of-the-art methods on next POI recommendation?
- **RQ2:** How do different designs of STAR-HiT influence the performance?
- **RQ3:** Can STAR-HiT capture the latent hierarchical structure present in check-in sequences?

In what follows, we first introduce datasets, evaluation metrics and compared methods, followed by answering the above questions. In particular, we present the performance comparison

with analysis among STAR-HiT and state-of-the-art baseline methods. Then, we explore how the hyper-parameter settings influence STAR-HiT, in terms of the initial length of subsequences, the number of stacked hierarchical encoders, the dimension of representations, *etc.* In addition, we examine the effect of different modules in STAR-HiT, in terms of four layers in the proposed hierarchical encoder and the learnable localization of subsequences. We also validate the capability of STAR-HiT to capture the personalized latent hierarchical structure of the check-in sequence by the case study.

4.1 Experimental Settings

4.1.1 Datasets

To evaluate the effectiveness of STAR-HiT, we conduct experiments on three publicly available datasets: Foursquare NYC, Foursquare US, and Gowalla.

- **Foursquare NYC:** Foursquare NYC [61] is a widely used dataset for POI recommendation, which contains check-ins in New York city collected from April 2012 to February 2013.
- **Foursquare US:** This dataset is a subset of a long-term global-scale check-in dataset collected from Foursquare [62]. Following [8], we use check-in data within the United States (except Alaska and Hawaii), and rename the dataset as Foursquare US.
- **Gowalla:** This is a check-in dataset obtained from Gowalla [14] over the period of February 2009 to October 2010.

Table 2 summarizes the statistics of three datasets, where *Revisit Frequency* refers to the ratio of the total number of check-ins to the number of visited POIs of a user. As for *Revisit Ratio*, it depicts the ratio of the number of repeated check-ins for the same POIs to the total number of check-ins of a user. Both of the above metrics measure re-visits in the dataset, which is complementary information to the sparsity. We report the average Revisit Frequency and Revisit Ratio of all users.

For each dataset, we filter out users and POIs with fewer than 10 check-ins as previous work [8] did. For the check-in sequence of each user, we set the maximum sequence length as L_{max} . Then we slide the fixed-length window on the original check-in trajectory to obtain sequence slices when $L > L_{\text{max}}$, otherwise padding with zeros to the right to construct the sequence of length L_{max} . Since the number of users in Foursquare NYC is much smaller, L_{max} is set to 100 for Foursquare NYC and 128 for others. In order to simulate the real-world next POI recommendation scenario, we rank the check-in sequence of each user in chronological order and split the dataset into training (80%), validation (10%), and test (10%) sets.

4.1.2 Evaluation Metrics

To evaluate the performance of next POI recommendation methods, we adopt two widely used evaluation protocols for recommendation systems [63]: HR@K and NDCG@K. For each test sequence, we predict the probabilities of candidate POIs $p \in \mathcal{P}$ and recommend the top- K POIs. Hit Ratio (HR) measures

Table 2: Statistics of Datasets

	Foursquare NYC	Foursquare US	Gowalla
# users	1,083	30,410	51,989
# POIs	5,135	79,580	131,282
# check-ins	147,938	2,440,233	3,365,444
Avg. POIs per user	137	80	65
Avg. users per POI	29	31	26
Revisit Frequency	4.89	2.88	2.56
Revisit Ratio	36.45%	26.72%	28.06%
Sparsity	97.34%	99.90%	99.95%

whether the true next visiting POI is present on the top- K ranked list, while Normalized Discounted Cumulative Gain (NDCG) further emphasizes the position of the hit by assigning higher weights to hits at topper ranks. We set $K = 5$ and $K = 10$ and report the average metrics for all sequences in the test set.

4.1.3 Compared Methods

We compare our proposed STAR-HiT with a statistical model (MFLM), RNN-based models (GRU4Rec, Time-LSTM, STRNN, STGN), attention-based model (STAN), and Transformer-based models (SASRec, SSE-PT, TiSASRec, GeoSAN), as follows:

- **MFLM:** Most Frequented Location Model [14] is a statistical-based model, which calculates the probability of a user visiting the POI based on the statistics of her previous check-ins. It captures the periodic check-in habit of the user.
- **GRU4Rec:** GRU4Rec [20] models the user action sequence for session-based recommendation utilizing Gated Recurrent Unit (GRU), a variant of RNN. We adopt a two-layer GRU for modeling check-in sequences.
- **Time-LSTM:** Time-LSTM [21] is a variant of LSTM that improves the modeling of sequential patterns by explicitly incorporating time intervals with designed time gates. We adopt the third version proposed in the paper since it achieves the best performance in our experiments.
- **STRNN:** Spatial Temporal Recurrent Neural Networks [6] improves RNN for check-in sequence modeling by capturing local temporal and spatial contexts with time and distance transition matrices.
- **STGN:** Spatio-temporal Gated Network [7] extends the gating mechanism of LSTM with four spatial-temporal gates to capture the user’s both long-term and short-term space and time preference.
- **STAN:** Spatio-Temporal Attention Network [10] uses a bi-layer attention architecture to explicitly exploit point-to-point spatio-temporal correlations in check-in sequences, so that correlations of non-adjacent locations and non-consecutive check-ins are well incorporated for understanding user behavior.
- **SASRec:** Self-Attention based Sequential Recommendation [29] directly implement the Transformer [43] ar-

chitecture, taking advantage of the self-attention mechanism to adaptively assign high weights to relatively few but relevant actions for recommendations.

- **SSE-PT:** Personalized Transformer with Stochastic Shared Embeddings (SSE) regularization [32] extends SASRec by introducing personalization into the model. The usage of SSE regularization prevents the model from overfitting after leveraging user embeddings.
- **TiSASRec:** Time interval aware Self-Attention based Sequential Recommendation [31] extends SASRec by modeling both absolute positions of items and personalized time intervals between them in sequences.
- **GeoSAN:** Geography-aware sequential recommender based on the Self-Attention Network [9] explicitly utilizes the time of check-ins and GPS positions of POIs. In particular, a self-attention based geography encoder is designed to encode the geographical information of each POI in the sequence.

4.1.4 Implementation Details

We implement the compared methods following the original settings. It should be noted that the experimental results of STAN on Foursquare US and Gowalla are ignored, due to its extremely high memory usage for the distance matrix of all POIs in large-scale datasets. Besides, we remove the geography-aware negative sampler in GeoSAN for a fair comparison, as it is not performed by other methods. We employ the BPR loss [64] for optimizing the RNN-based models, since the cross-entropy loss generally leads to poor performance. As for our proposed STAR-HiT, the embedding dimension d is set to 68 and the hidden dimension d_k in the feed-forward networks is set to twice the embedding dimension, which is 128. The weights w^1, w^2 that control the offset and scale to update the subsequence location are both set to 1, and the dropout ratio is set to 0.2. Inspired by [43], we train the model using the Adam optimizer [65] with $\beta_1 = 0.9, \beta_2 = 0.98, \epsilon = 10^{-9}$, and the learning rate l_rate is varied over the course of training as: $\text{l_rate} = \lambda \cdot d^{-0.5} \cdot \min(\text{num_step}^{-0.5}, \text{num_step} \cdot \text{warmup_step}^{-1.5})$, where d is the embedding dimension, num_step is the number of training steps, the coefficient λ controls the overall learning rate which is set to 1, warmup_step refers to the training step with the peak learning rate and is set to 400. We use the Xavier initialization [66] to initialize model parameters. For all models, we use the default number of training epochs of 200 for Foursquare NYC and 300 for others, and the default mini-batch size of

128. Our model is implemented in PyTorch and available at <https://github.com/JennyXieJiayi/STAR-HiT>.

4.2 Performance Comparison (RQ1)

The performance comparison with baseline methods are illustrated in Table 3. We have the following observations:

- The proposed STAR-HiT achieves the best performance among all the compared methods. In particular, STAR-HiT improves the performance over the strongest baseline, *i.e.*, GeoSAN, in terms of HR@5 by 23.6%, 69.94%, 34.29% in Foursquare NYC, Foursquare US, and Gowalla, respectively. Moreover, the corresponding performance improvements in terms of NDCG@5 are 52.69%, 95.58%, and 51.79%, respectively. By stacked hierarchical encoders, STAR-HiT benefits from spatio-temporal context modeling and multi-granularity semantic subsequences discovering in an explicit manner, so as to model the inherent hierarchical structure exhibited in check-in sequences. This verifies the significance of modeling the hierarchical structure of check-in sequences to improve the recommendations.
- The statistical model MFLM achieves relatively poor performance on Foursquare US and Gowalla, while performing comparable to RNN-based models (*i.e.*, GRU4Rec, Time-LSTM, STRNN, STGN) on Foursquare NYC. The reason may lie in that there are more revisits for users in Foursquare NYC than others (*cf.* Table 2). Combining the subtle differences of MFLM performing in terms of HRs and NDCGs, we can conclude that MFLM is suitable for users with periodic check-in patterns, while unable to deal with those with a certain degree of flexible check-in patterns.
- STAN and Transformer-based models (*i.e.*, SASRec, SSE-PT, TiSASRec, GeoSAN, STAR-HiT) with the self-attention mechanism as the major component, consistently outperform RNN-based models. The recurrent neural networks handle the check-in sequence by recursively encoding previous check-ins into the internal memory as a whole, such that correlations between non-consecutive check-ins and long-term semantics are underestimated. Instead, the self-attention mechanism allows capturing the correlations of any two check-ins in an explicit way, despite whether they are consecutive.
- Among RNN-based methods, models that consider at least one of the spatial and temporal contexts (*i.e.*, Time-LSTM, STRNN, STGN) perform better than others (*i.e.*, GRU4Rec). Likewise, GeoSAN and STAR-HiT that embed the spatio-temporal context outperform SASRec, SSE-PT, and TiSASRec designed for traditional items. These results highlight the importance of spatio-temporal context modeling.

4.3 Study of STAR-HiT (RQ2)

To get deep insights into the design of STAR-HiT, we first explore how different settings influence the performance, in terms

of the initial length of subsequences, the number of stacked hierarchical encoders, the embedding dimension. Then, we analyze the effectiveness of the various components by conducting an ablation study.

4.3.1 Parameter Analysis

The initial length of subsequences and the number of stacked hierarchical encoders play critical roles in STAR-HiT. For example, one-encoder model is unable to capture the hierarchical structure of the check-in sequence, while the semantic subsequences can hardly be discovered if the initial length of subsequences are set too short. On the contrary, too much encoders could lead to an overfitting issue. Besides, if the initial subsequence length is set too long, check-ins with low correlation are aggregated together, which could introduce unwanted noises. Therefore, it is reasonable to assume that there exist optimal settings of these two hyper-parameters for latent hierarchical structure modeling of check-in sequences. Towards this end, we perform experiments with different settings of these two hyper-parameters to investigate their impact on performance. Specifically, we vary the number of hierarchical encoders (*i.e.*, l) in $\{1, 2, 3\}$ and the initial subsequence length (*i.e.*, k) in $\{1, 2, 4, 6, 8, 10, 12\}$. We use STAR-HiT _{l,k} to denote the STAR-HiT with l hierarchical encoders while the initial subsequence length is set to j . The experimental results are summarized in Figure 3, where lines represent the results *w.r.t.* $K = 5$ and bars in same color depict results *w.r.t.* $K = 10$ for corresponding settings. From this result, we have the following observations:

- STAR-HiT_{2,8} yields the best performance across all the board. Therefore, we set $l = 2, k = 8$ as default parameters unless otherwise specified. This verifies that STAR-HiT benefits from appropriate settings of l and k to effectively model the latent hierarchical structure of check-in sequences, so as to achieve superior recommendation performance.
- With fixed l , the performance first increases then drops as k gets larger in most cases. Moreover, with larger l , the performance is more likely to peak at smaller k . It is also worthwhile to note that on Foursquare NYC and Foursquare US, STAR-HiT_{2, k} performs worse than STAR-HiT_{3, k} when $k < 6$, while outperforms STAR-HiT_{3, k} when $k \leq 6$. We attribute these characteristics to the similar role the two parameters play in capturing the multi-granularity semantic subsequences.
- STAR-HiT_{1, k} performs worst compared to STAR-HiT_{2, k} or STAR-HiT_{3, k} on Foursquare NYC generally. The reason may lie in the relatively high revisit frequency in Foursquare NYC that exhibits a stronger hierarchical structure of the check-in sequence.
- STAR-HiT_{3, k} falls behind STAR-HiT_{1, k} or STAR-HiT_{2, k} by a large margin in most cases on Gowalla. The possible reasons are two-fold, that is, the low revisit frequency and the high sparsity lead to difficulties in capturing the hierarchical structure of check-in sequences.

Taking Foursquare NYC as an example, we analyze the training efficiency of STAR-HiT with different settings of l and k .

Table 3: Performance Comparison with Baseline Methods

	Foursquare NYC				Foursquare US				Gowalla			
	H@5	H@10	N@5	N@10	H@5	H@10	N@5	N@10	H@5	H@10	N@5	N@10
MFLM	0.1412	0.1421	0.1316	0.1319	0.1386	0.1394	0.1296	0.1299	0.1176	0.1176	0.1106	0.1106
GRU4Rec	0.1421	0.2335	0.1006	0.1310	0.1412	0.1908	0.1074	0.1227	0.1459	0.1983	0.1057	0.1227
Time-LSTM	0.1584	0.2534	0.1085	0.1429	0.1426	0.1928	0.1091	0.1247	0.1465	0.2002	0.1076	0.1243
STRNN	0.1475	0.2425	0.1006	0.1317	0.1738	0.2424	0.1314	0.1533	0.1474	0.2045	0.1078	0.1250
STGN	0.1548	0.2561	0.1132	0.1452	0.1803	0.2538	0.1341	0.1588	0.1467	0.2088	0.1070	0.1264
STAN	0.3587	0.5112	0.2506	0.3008	-	-	-	-	-	-	-	-
SASRec	0.3439	0.4597	0.1719	0.1882	0.2727	0.3765	0.1276	0.1356	0.2550	0.3635	0.1169	0.1253
SSE-PT	0.3719	0.4950	0.2362	0.2751	0.3181	0.3829	0.2029	0.2056	0.3049	0.4050	0.1596	0.1667
TiSASRec	0.3665	0.4860	0.2621	0.3008	0.2803	0.3834	0.1419	0.1491	0.2926	0.3851	0.1462	0.1522
GeoSAN	0.4847	0.5571	0.3396	0.3630	0.4100	0.4991	0.3263	0.3551	0.3349	0.4183	0.2583	0.2855
STAR-HiT	0.5991	0.6597	0.5186	0.5385	0.6968	0.7296	0.6381	0.6486	0.4497	0.4929	0.3921	0.4057
<i>Improv.</i>	23.60%	18.42%	52.69%	48.32%	69.94%	46.18%	95.58%	82.65%	34.29%	17.82%	51.79%	42.13%

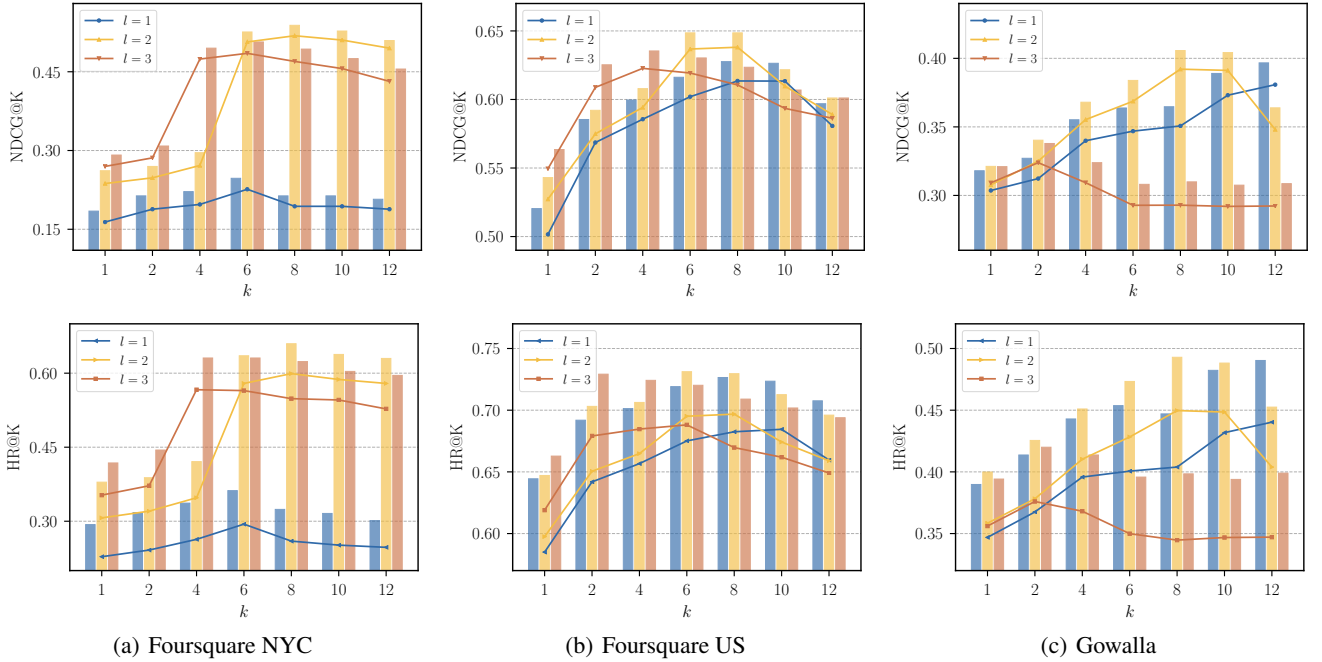


Figure 3: Parameter analysis on three datasets.

The training loss curves are illustrated in Figure 4. As we can see, STAR-HiT_{1:1} and STAR-HiT_{2:1} exhibit large fluctuations compared to models with higher k . When $l = 1$, the training loss curve of STAR-HiT_{1:4} is generally lower and more stable than STAR-HiT_{1:8} and STAR-HiT_{1:12}, while such differences are unnoticeable when $l = 2$. In addition, when $k > 1$, the loss of STAR-HiT_{2:k} drops faster and more steadily to nearly zero compared to STAR-HiT_{1:k}. Jointly analyzing Figure 3 and Figure 4, we again verify that with the suitable settings of l and k , STAR-HiT is capable of discovering the semantic subsequences in check-in sequences, thereby better uncovering the hierarchical structure present in user sequential behavior patterns.

4.3.2 Effect of the embedding dimension

We also conduct experiments to analyze the effect of the embedding dimension (*i.e.*, d) used in STAR-HiT. In particular, we set the embedding dimension from 16 to 112, with a step

of 16. Figure 5 illustrates the experimental results in terms of NDCG@10 and HR@10 on three datasets. From Figure 5, we can see that the performance gets much worse when using a small embedding dimension, as it is insufficient to encode the contextual information. As the embedding dimension grows, the performance first increases dramatically and then gradually becomes stable. Considering the trade-off between cost and performance, we set the default embedding dimension d to 64.

4.3.3 Ablation Study

As stated, there are two essential components of the proposed hierarchical encoder, including: 1) **attention module**, including the global attention layer and local attention layer, which captures global context and local context to enhance representations; 2) **subsequence aggregation module**, including the sequence partition layer and subsequence aggregation layer, which utilizes contextual information to reason and locate subsequences,

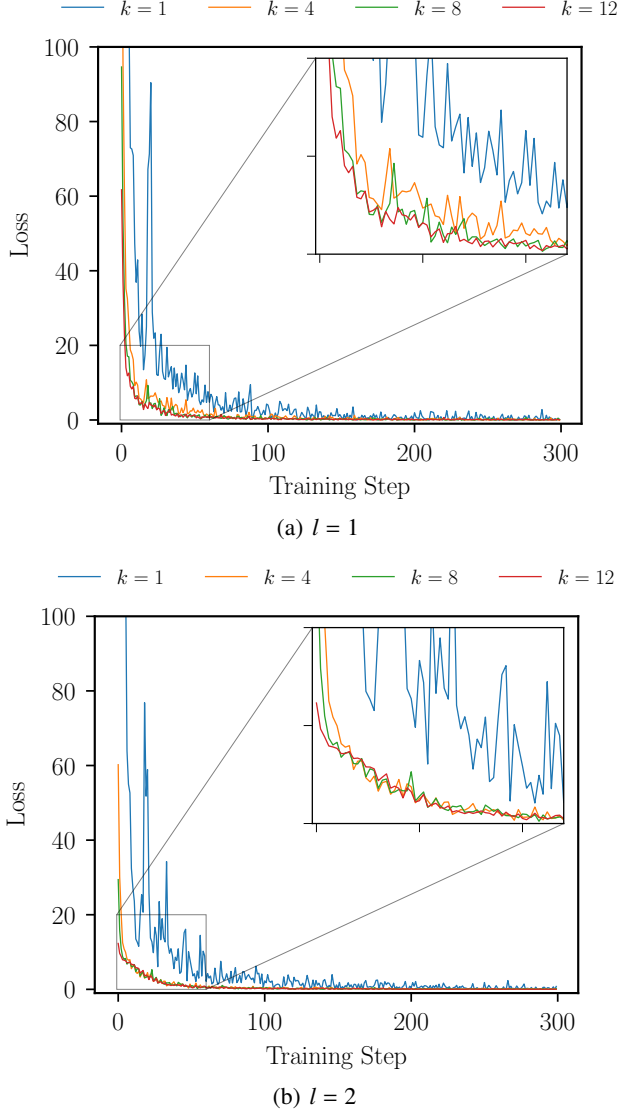


Figure 4: Training efficiency on Foursquare NYC with different initial subsequence lengths k .

thereby obtaining semantic subsequences. To analyze the effectiveness of the various components, we conduct an ablation study by considering the following variants:

- **STAR-HiT_{GA}**: The global attention layer in each hierarchical encoder is removed, which captures the global spatio-temporal context to enhance representations.
- **STAR-HiT_{LA}**: The local attention layer in each hierarchical encoder is removed, which injects the local context of the extracted subsequence into each representations within.
- **STAR-HiT_{LGA}**: Both the global attention layer and local attention layer are removed, such that the model solely hierarchically partitions the sequence and aggregates the subsequences without any contextual enhancement.

- **STAR-HiT_{AGG2}**: The hierarchical structure modeling through the sequence partition layer and subsequence aggregation layer is disabled. The local attention layer is removed as well, since it is calculated within the identified subsequence. Overall, the proposed hierarchical encoder degrades to the vanilla Transformer encoder that solely learns from POI-to-POI interactions.
- **STAR-HiT_{AGG4}**: Since there are two attention layers in a hierarchical encoder, we also double the number of encoders (*i.e.*, $l = 4$) for STAR-HiT_{AGG2}, so as to involve the same number of attention layers as the original STAR-HiT.

Table 4 compares the performance of STAR-HiT and its variants in terms of NDCG@5 and NDCG@10. From Table 4, we have three key observations:

- **Attention module**: Removing the global attention layer leads to significant performance drops in terms of NDCG@5 by 12.05%-33.86% and NDCG@10 by 11.26%-33.11% on three datasets. Besides, removing the local attention layer leads to relatively slight performance drops with regard to NDCG@5 by 2.63%-9.08% and NDCG@10 by 2.23%-8.74%. Since the local attention is calculated within each extracted subsequence, it may be affected by the performance of the subsequence partition layer. This may be the reason why the local attention layer provides less performance improvement compared to the global attention layer. Overall, jointly removing the attention module makes the model unable to make full use of the context, resulting in even worse performance, that is, the performance drops in terms of NDCG@5 by 16.01%-41.01% and NDCG@10 by 15.11%-41.34%.
- **Subsequence aggregation module**: Disabling the multi-granularity subsequence aggregation, STAR-HiT_{AGG2} performs 11.78%-63.00%, 10.75%-60.00% worse than STAR-HiT in terms of NDCG@5, NDCG@10, respectively. STAR-HiT_{AGG4} yields worse performance as well. Surprisingly, STAR-HiT_{AGG4} outperforms STAR-HiT_{AGG2} on Foursquare NYC, while performs notably worse on others. The results indicate that STAR-HiT_{AGG4} may suffer from overfitting issue due to the sparsity of data. The performance comparison demonstrates the significance of involving not only POI-to-POI interactions but also subsequence-level context and interactions for recommendations, which is achieved by STAR-HiT.
- As expected, STAR-HiT outperforms all the variants by a large margin. Moreover, jointly analyzing Table 3 and Table 4, we can see that the variants of STAR-HiT still achieve competitive performance compared to baseline methods. The results emphasize the significance of joint context modeling through attention mechanisms and hierarchical structure modeling through multi-granularity semantic subsequence discovering.

The sequence partition layer in the hierarchical encoder adaptively partitions the input sequence into multiple semantic subsequences, wherein the offset (*i.e.*, dx_i) and length (*i.e.*, k_i) for each

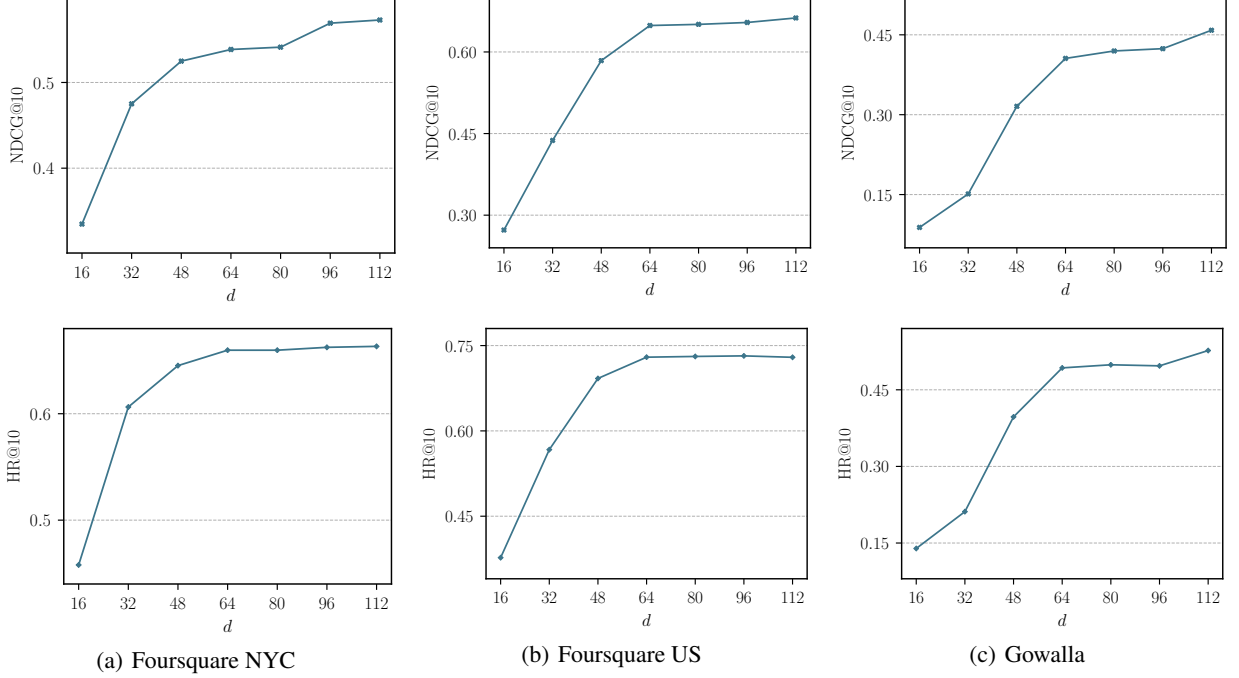
Figure 5: Effect of the embedding dimension d .

Table 4: Performance Comparison (NDCG@K) with STAR-HiT Variants

	Foursquare NYC		Foursquare US		Gowalla	
	NDCG@5	NDCG@10	NDCG@5	NDCG@10	NDCG@5	NDCG@10
STAR-HiT _{GA}	0.3430	0.3602	0.5612	0.5756	0.2988	0.3162
STAR-HiT _{LA}	0.4715	0.4914	0.6213	0.6341	0.3569	0.3728
STAR-HiT _{GLA}	0.3059	0.3158	0.5359	0.5505	0.2825	0.2970
STAR-HiT _{AGG2}	0.1919	0.2154	0.5457	0.5608	0.3459	0.3621
STAR-HiT _{AGG4}	0.2136	0.2326	0.3540	0.3729	0.2556	0.2651
STAR-HiT	0.5186	0.5385	0.6381	0.6486	0.3921	0.4057

subsequence are learned. Offsets are predicted to shift the subsequences towards check-ins with strong correlation, whereas lengths are utilized to better maintain local semantics. They are both supposed to facilitate the performance of STAR-HiT.

Accordingly, we conduct experiments to explore how the learnable subsequence locations affect the performance. In particular, we implement the variants of STAR-HiT, STAR-HiT_{GA}, STAR-HiT_{LA}, STAR-HiT_{GLA} by disabling the learnable offsets and lengths, that is, subsequences are fixed to be extracted by uniformly partitioning the input sequence. We denote these variants as STAR-HiT_F, STAR-HiT_{GA-F}, STAR-HiT_{LA-F}, and STAR-HiT_{GLA-F}, respectively. The experimental results in terms of NDCG@5 and NDCG@10 are shown in Table 5. In general, models with learnable locations of subsequences improve over models with fixed-length subsequence extraction by 64.87%-126.95%, 5.40%-14.24%, 4.82%-9.91% in terms of NDCG@5, and 89.67%-97.03%, 4.63%-12.52%, 4.82%-10.57% in terms of NDCG@10 on three datasets. It is worth noting that learnable locations of subsequence boost the performance substantially in Foursquare NYC. This may be due to the stronger hierarchi-

cal structure present in check-in sequences in Foursquare NYC, which is consistent with the findings in Section 4.3.1. Partitioning the sequence into subsequences in a fixed way could potentially destroy the semantic information, eventually resulting in the failure to capture the hierarchical structure in check-in sequences. By adaptively partition the sequence into subsequences with different positions and lengths learned from contextual information, STAR-HiT is able to model the hierarchical structure of the check-in sequence by well preserving the semantics in subsequences.

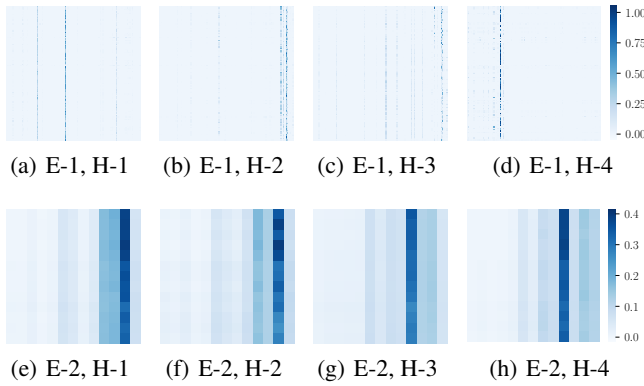
4.4 Case Study (RQ3)

Jointly modeling the spatio-temporal context and multi-granularity semantic subsequences, STAR-HiT makes full use of the personalized sequential behavior pattern to predict the next visiting POI. In order to better understand the capability of STAR-HiT to model the latent hierarchical structure, we randomly select a check-in sequence sample (*uid*: 172) on the test set from Foursquare NYC to conduct a case study.

Table 5: Performance Comparison (NDCG@K) with STAR-HiT Variants of Fixed-Length Subsequences

	Foursquare NYC		Foursquare US		Gowalla	
	NDCG@5	NDCG@10	NDCG@5	NDCG@10	NDCG@5	NDCG@10
STAR-HiT _{GA}	0.3430	0.3602	0.5612	0.5756	0.2988	0.3162
STAR-HiT _{GA-F}	0.1511	0.1828	0.5296	0.5487	0.2719	0.2860
STAR-HiT _{LA}	0.4715	0.4914	0.6213	0.6341	0.3569	0.3728
STAR-HiT _{LA-F}	0.2860	0.3050	0.5439	0.5635	0.3405	0.3556
STAR-HiT _{GLA}	0.3059	0.3158	0.5359	0.5505	0.2825	0.2970
STAR-HiT _{GLA-F}	0.1430	0.1665	0.5085	0.5262	0.2612	0.2758
STAR-HiT	0.5186	0.5385	0.6381	0.6486	0.3921	0.4057
STAR-HiT _F	0.3014	0.3240	0.5686	0.5874	0.3247	0.3411

We first visualize the global attention weights of each head in each encoder to validate the capacity of STAR-HiT to encode spatio-temporal context. As shown in Figure 6, different heads in Encoder-1 highlight different relevant check-ins, whereas heads in Encoder-2 after a round of subsequence aggregation consistently focus on the last few check-in subsequences, which seems to be the most representative subsequences correlated to the target check-in. Encoder-1 is responsible for encoding the correlations between individual check-ins, thus check-ins to the same POI or with similar spatio-temporal context to the target check-in are most likely to be assigned high weights. Note that even the weights of different check-ins to the same POI are not identical, due to the spatio-temporal context embedding that makes representations position-specific. Next, Encoder-2 focuses on subsequence-level correlation, thus the most relevant subsequences generally point to recent subsequences with similar periodicity.

Figure 6: Heatmaps of global attention weights of a random sample (*uid*: 172) from Foursquare NYC.

In addition, we visualize the correlation matrix $M \in \mathbb{R}^{L \times L}$ of check-in representations to validate the effectiveness of STAR-HiT in capturing the latent hierarchical structure of the check-in sequence. The final check-in representations are obtained by: 1) concatenating the context-aware representations $\mathbf{E}(u)$ and their belonging subsequence representations in each encoder, 2) calculating the Pearson Correlation Coefficient (PCC) of normalized representations of i -th check-in and j -th check-in, which serve as each element $M_{i,j}$ in the correlation matrix. The correlation

matrix is illustrated in Figure 7(a), and meanwhile the check-in sequence segment corresponding to the region marked with the red-dotted rectangle is shown in 7(b). We also plot the visited POIs projected on the map in Figure 7(c). From Figure 7, we can see that STAR-HiT uncovers the multi-granularity semantic subsequences. For daily regularity, check-ins on Tuesday (*pid*: 8, 16, 5) are identified as a subsequence, while the check-ins from Tuesday noon to Wednesday noon (*pid*: 8, 16, 5, 3, 2, 1) are extracted as another subsequence. Furthermore, the weekly regularity is discovered as well, that is, the first week marked with the red-dotted rectangle in 7(a) is clearly separated from the following weeks. It should be noted that as shown in Figure 7(b), some subsequences aggregate the last check-in (*pid*: 5) with former check-ins while some do not. It is reasonable since that even though the check-in of POI 5 occurs on Monday, it occurs in the early hours of Monday, so it is more likely to be on the same itinerary as the previous check-in.

Overall, the proposed STAR-HiT can not only achieve superior recommendation performance, but also effectively capture the latent hierarchical structure present in check-in sequences, thereby providing explanations for personalized recommendations accordingly.

5 CONCLUSION

In this work, we explore the latent hierarchical structure of sequential behavior patterns exhibited in user movements. We propose a novel Spatio-Temporal context AggRegated Hierarchical Transformer (STAR-HiT) model for next POI recommendation, which consists of stacked hierarchical encoders to capture the latent hierarchical structure of check-in sequences. Specifically, the hierarchical encoder is designed to jointly model spatio-temporal context and locate semantic subsequences with different positions and lengths in an explicit way. In each encoder, the global and local attention layers enhance spatio-temporal context modeling by capturing inter- and intra- subsequence dependencies; meanwhile, the sequence partition layer and subsequence aggregation layer adaptively locate and fuse semantic subsequences, and generate a new sequence with a higher level of granularity. This sequence is then fed into the next encoder for further subsequence discovery and sequence abstraction. By stacking multiple hierarchical encoders, semantic subsequences of different granularities are recursively identified and integrated,

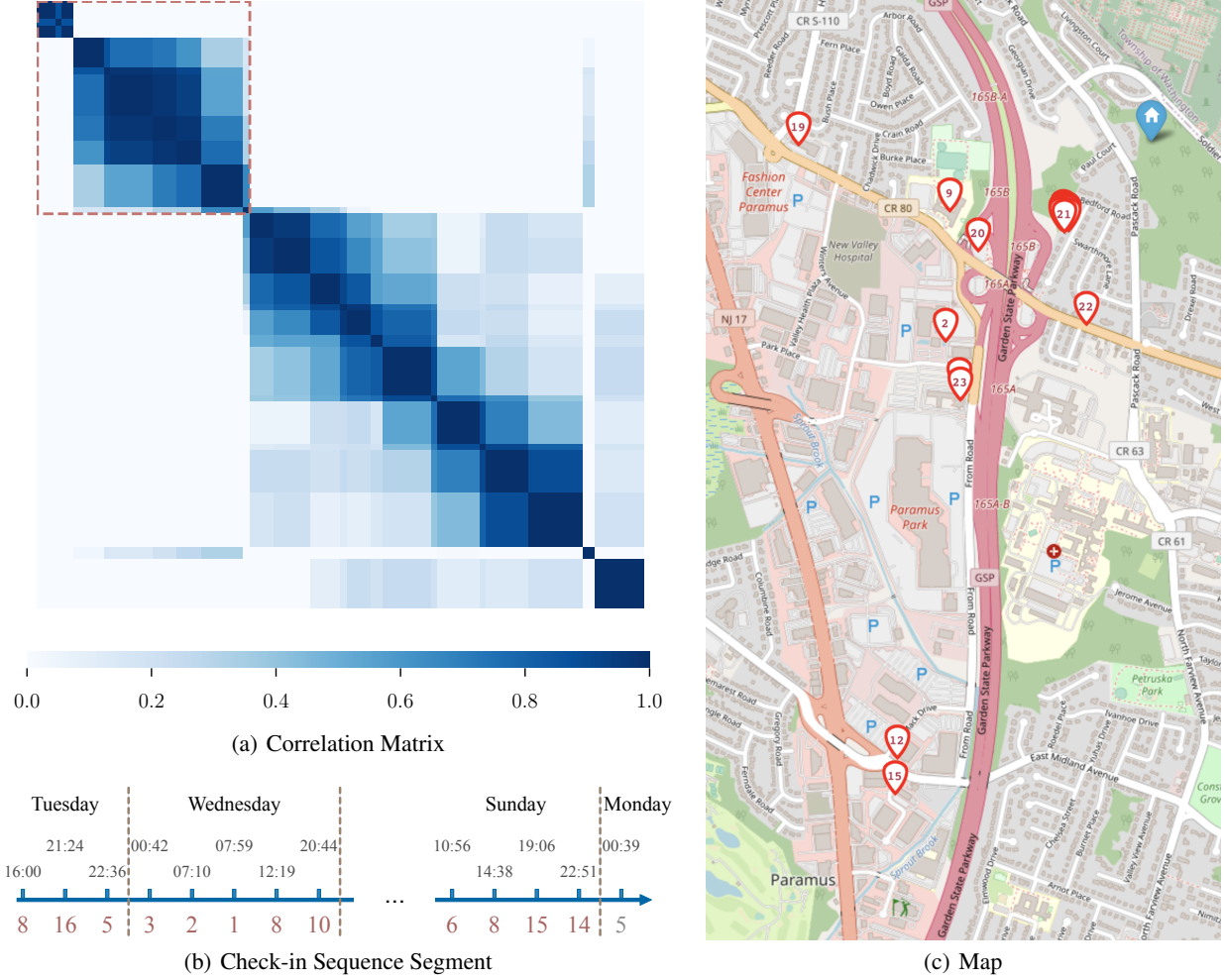


Figure 7: Visualization of a random sample (*uid*: 172) on the test set.

constituting the overall hierarchical structure present in the user movement. We perform extensive experiments on three public datasets to: 1) demonstrate that our proposed STAR-HiT outperforms state-of-the-art methods by a large margin, 2) get deep insights into the design of STAR-HiT, and 3) verify that STAR-HiT successfully captures multi-level semantic subsequences for revealing the latent hierarchical structure of the check-in sequence, so as to guarantee the robustness and explainability of the recommendation.

REFERENCES

- [1] Hossein A. Rahmani, Mohammad Aliannejadi, Mitra Baratchi, and Fabio Crestani. A systematic analysis on the impact of contextual information on point-of-interest recommendation. *ACM Trans. Inf. Syst.*, 40(4):88:1–88:35, 2022. URL <https://doi.org/10.1145/3508478>.
- [2] Md. Ashraful Islam, Mir Mahathir Mohammad, Sarkar Snigdha Sarathi Das, and Mohammed Eunus Ali. A survey on deep learning based point-of-interest (POI) recommendations. *Neurocomputing*, 472:306–325, 2022. URL <https://doi.org/10.1016/j.neucom.2021.05.114>.
- [3] Chen Cheng, Haiqin Yang, Michael R. Lyu, and Irwin King. Where you like to go next: Successive point-of-interest recommendation. In *Proceedings of the 23rd International Joint Conference on Artificial Intelligence (IJCAI ’13)*, pages 2605–2611, 2013. URL <https://ijcai.org/Abstract/13/384>.
- [4] Shanshan Feng, Xutao Li, Yifeng Zeng, Gao Cong, Yeow Meng Chee, and Quan Yuan. Personalized ranking metric embedding for next new POI recommendation. In *Proceedings of the 24th International Joint Conference on Artificial Intelligence (IJCAI ’15)*, pages 2069–2075, 2015. URL <http://ijcai.org/Abstract/15/293>.
- [5] Tomás Mikolov, Ilya Sutskever, Kai Chen, Gregory S. Corrado, and Jeffrey Dean. Distributed representations of words and phrases and their compositionality. In *Proceedings of the Advances in Neural Information Processing Systems (NeurIPS ’13)*, pages 3111–3119, 2013. URL <https://proceedings.neurips.cc/paper/2013/file/9aa42b31882ec039965f3c4923ce901b-Paper.pdf>.

- [6] Qiang Liu, Shu Wu, Liang Wang, and Tieniu Tan. Predicting the next location: A recurrent model with spatial and temporal contexts. In *Proceedings of the 30th AAAI Conference on Artificial Intelligence (AAAI '16)*, pages 194–200, 2016. URL <https://ojs.aaai.org/index.php/AAAI/article/view/9971>.
- [7] Pengpeng Zhao, Haifeng Zhu, Yanchi Liu, Jiajie Xu, Zhixu Li, Fuzhen Zhuang, Victor S. Sheng, and Xiaofang Zhou. Where to go next: A spatio-temporal gated network for next POI recommendation. In *Proceedings of the 33th AAAI Conference on Artificial Intelligence (AAAI '19)*, pages 5877–5884, 2019. URL <https://doi.org/10.1609/aaai.v33i01.33015877>.
- [8] Kangzhi Zhao, Yong Zhang, Hongzhi Yin, Jin Wang, Kai Zheng, Xiaofang Zhou, and Chunxiao Xing. Discovering subsequence patterns for next POI recommendation. In *Proceedings of the 29th International Joint Conference on Artificial Intelligence (IJCAI '20)*, pages 3216–3222, 2020. URL <https://doi.org/10.24963/ijcai.2020/445>.
- [9] Defu Lian, Yongji Wu, Yong Ge, Xing Xie, and Enhong Chen. Geography-aware sequential location recommendation. In *Proceedings of the 26th ACM SIGKDD Conference on Knowledge Discovery and Data Mining (KDD '20)*, pages 2009–2019, 2020. URL <https://doi.org/10.1145/3394486.3403252>.
- [10] Yingtao Luo, Qiang Liu, and Zhaocheng Liu. STAN: spatio-temporal attention network for next location recommendation. In *Proceedings of the Web Conference (WWW '21)*, pages 2177–2185, 2021. URL <https://doi.org/10.1145/3442381.3449998>.
- [11] Xiao Zhou, Cecilia Mascolo, and Zhongxiang Zhao. Topic-enhanced memory networks for personalised point-of-interest recommendation. In *Proceedings of the 25th ACM SIGKDD International Conference on Knowledge Discovery & Data Mining (KDD '19)*, pages 3018–3028, 2019. URL <https://doi.org/10.1145/3292500.3330781>.
- [12] Yan Lin, Huaiyu Wan, Shengnan Guo, and Youfang Lin. Pre-training context and time aware location embeddings from spatial-temporal trajectories for user next location prediction. In *Proceedings of the 35th AAAI Conference on Artificial Intelligence (AAAI '21)*, pages 4241–4248, 2021. URL <https://ojs.aaai.org/index.php/AAAI/article/view/16548>.
- [13] Yudong Chen, Xin Wang, Miao Fan, Jizhou Huang, Shengwen Yang, and Wenwu Zhu. Curriculum meta-learning for next POI recommendation. In *Proceedings of the 27th ACM SIGKDD Conference on Knowledge Discovery and Data Mining (KDD '21)*, pages 2692–2702, 2021. URL <https://doi.org/10.1145/3447548.3467132>.
- [14] Eunjoon Cho, Seth A. Myers, and Jure Leskovec. Friendship and mobility: User movement in location-based social networks. In *Proceedings of the 17th ACM SIGKDD International Conference on Knowledge Discovery and Data Mining (KDD '11)*, pages 1082–1090, 2011. URL <https://doi.org/10.1145/2020408.2020579>.
- [15] Steffen Rendle, Christoph Freudenthaler, and Lars Schmidt-Thieme. Factorizing personalized markov chains for next-basket recommendation. In *Proceedings of the 19th International Conference on World Wide Web (WWW '10)*, pages 811–820, 2010. URL <https://doi.org/10.1145/1772690.1772773>.
- [16] Ruining He and Julian J. McAuley. Fusing similarity models with markov chains for sparse sequential recommendation. In *Proceedings of the 16th IEEE International Conference on Data Mining (ICDM '16)*, pages 191–200, 2016. URL <https://doi.org/10.1109/ICDM.2016.0030>.
- [17] Ruining He, Wang-Cheng Kang, and Julian J. McAuley. Translation-based recommendation. In *Proceedings of the 11th ACM Conference on Recommender Systems (RecSys '17)*, pages 161–169, 2017. URL <https://doi.org/10.1145/3109859.3109882>.
- [18] Jiaxi Tang and Ke Wang. Personalized top-n sequential recommendation via convolutional sequence embedding. In *Proceedings of the 11th ACM International Conference on Web Search and Data Mining (WSDM '18)*, pages 565–573, 2018. URL <https://doi.org/10.1145/3159652.3159656>.
- [19] Fajie Yuan, Alexandros Karatzoglou, Ioannis Arapakis, Joemon M. Jose, and Xiangnan He. A simple convolutional generative network for next item recommendation. In *Proceedings of the 12th ACM International Conference on Web Search and Data Mining (WSDM '19)*, pages 582–590, 2019. URL <https://doi.org/10.1145/3289600.3290975>.
- [20] Balázs Hidasi, Alexandros Karatzoglou, Linas Baltrunas, and Domonkos Tikk. Session-based recommendations with recurrent neural networks. In *Proceedings of the 4th International Conference on Learning Representations (ICLR '16)*, 2016. URL <http://arxiv.org/abs/1511.06939>.
- [21] Yu Zhu, Hao Li, Yikang Liao, Beidou Wang, Ziyu Guan, Haifeng Liu, and Deng Cai. What to do next: Modeling user behaviors by time-lstm. In *Proceedings of the 26th International Joint Conference on Artificial Intelligence (IJCAI '17)*, pages 3602–3608, 2017. URL <https://doi.org/10.24963/ijcai.2017/504>.
- [22] Chengfeng Xu, Pengpeng Zhao, Yanchi Liu, Victor S. Sheng, Jiajie Xu, Fuzhen Zhuang, Junhua Fang, and Xiaofang Zhou. Graph contextualized self-attention network for session-based recommendation. In *Proceedings of the 28th International Joint Conference on Artificial Intelligence (IJCAI '19)*, pages 3940–3946, 2019. URL <https://doi.org/10.24963/ijcai.2019/547>.
- [23] Shu Wu, Yuyuan Tang, Yanqiao Zhu, Liang Wang, Xing Xie, and Tieniu Tan. Session-based recommendation with graph neural networks. In *Proceedings of the 33rd AAAI Conference on Artificial Intelligence (AAAI '19)*, pages 346–353, 2019. URL <https://doi.org/10.1609/aaai.v33i01.3301346>.
- [24] Haochao Ying, Fuzhen Zhuang, Fuzheng Zhang, Yanchi Liu, Guandong Xu, Xing Xie, Hui Xiong, and Jian Wu. Sequential recommender system based on hierarchical attention networks. In *Proceedings of the 27th International Joint Conference on Artificial Intelligence (IJCAI '18)*,

- pages 3926–3932, 2018. URL <https://doi.org/10.24963/ijcai.2018/546>.
- [25] Jin Huang, Wayne Xin Zhao, Hongjian Dou, Ji-Rong Wen, and Edward Y. Chang. Improving sequential recommendation with knowledge-enhanced memory networks. In *Proceedings of the 41st International ACM SIGIR Conference on Research & Development in Information Retrieval (SIGIR '18)*, pages 505–514, 2018. URL <https://doi.org/10.1145/3209978.3210017>.
- [26] Zhenlei Wang, Jingsen Zhang, Hongteng Xu, Xu Chen, Yongfeng Zhang, Wayne Xin Zhao, and Ji-Rong Wen. Counterfactual data-augmented sequential recommendation. In *Proceedings of the 44th International ACM SIGIR Conference on Research and Development in Information Retrieval (SIGIR '21)*, pages 347–356, 2021. URL <https://doi.org/10.1145/3404835.3462855>.
- [27] Kun Zhou, Hui Yu, Wayne Xin Zhao, and Ji-Rong Wen. Filter-enhanced MLP is all you need for sequential recommendation. In *Proceedings of the ACM Web Conference (WWW '22)*, pages 2388–2399, 2022. URL <https://doi.org/10.1145/3485447.3512111>.
- [28] Shuqing Bian, Wayne Xin Zhao, Kun Zhou, Xu Chen, Jing Cai, Yancheng He, Xingji Luo, and Ji-Rong Wen. A novel macro-micro fusion network for user representation learning on mobile apps. In *Proceedings of the Web Conference (WWW '21)*, pages 3199–3209, 2021. URL <https://doi.org/10.1145/3442381.3450109>.
- [29] Wang-Cheng Kang and Julian J. McAuley. Self-attentive sequential recommendation. In *Proceedings of the IEEE International Conference on Data Mining (ICDM '18)*, pages 197–206, 2018. URL <https://doi.org/10.1109/ICDM.2018.00035>.
- [30] Fei Sun, Jun Liu, Jian Wu, Changhua Pei, Xiao Lin, Wenwu Ou, and Peng Jiang. Bert4rec: Sequential recommendation with bidirectional encoder representations from transformer. In *Proceedings of the 28th ACM International Conference on Information and Knowledge Management (CIKM '19)*, pages 1441–1450, 2019. URL <https://doi.org/10.1145/3357384.3357895>.
- [31] Jiacheng Li, Yujie Wang, and Julian J. McAuley. Time interval aware self-attention for sequential recommendation. In *Proceedings of the 13th ACM International Conference on Web Search and Data Mining (WSDM '20)*, pages 322–330, 2020. URL <https://doi.org/10.1145/3336191.3371786>.
- [32] Liwei Wu, Shuqing Li, Cho-Jui Hsieh, and James Sharpnack. SSE-PT: sequential recommendation via personalized transformer. In *Proceedings of ACM Conference on Recommender Systems (RecSys '20)*, pages 328–337, 2020. URL <https://doi.org/10.1145/3383313.3412258>.
- [33] Zhiwei Liu, Ziwei Fan, Yu Wang, and Philip S. Yu. Augmenting sequential recommendation with pseudo-prior items via reversely pre-training transformer. In *Proceedings of the 44th International ACM SIGIR Conference on Research and Development in Information Retrieval (SIGIR '21)*, pages 1608–1612, 2021. URL <https://doi.org/10.1145/3404835.3463036>.
- [34] Jing He, Xin Li, Lejian Liao, Dandan Song, and William K. Cheung. Inferring a personalized next point-of-interest recommendation model with latent behavior patterns. In *Proceedings of the 30th AAAI Conference on Artificial Intelligence (AAAI '16)*, pages 137–143, 2016. URL <https://doi.org/10.1609/aaai.v30i1.9994>.
- [35] Shanshan Feng, Gao Cong, Bo An, and Yeow Meng Chee. Poi2vec: Geographical latent representation for predicting future visitors. In *Proceedings of the 31st AAAI Conference on Artificial Intelligence (AAAI '17)*, pages 102–108, 2017. URL <https://doi.org/10.1609/aaai.v31i1.10500>.
- [36] Shenglin Zhao, Tong Zhao, Irwin King, and Michael R. Lyu. Geo-teaser: Geo-temporal sequential embedding rank for point-of-interest recommendation. In *Proceedings of the 26th International Conference on World Wide Web Companion (WWW '17 Companion)*, volume 26, pages 153–162, 2017. URL <https://doi.org/10.1145/3041021.3054138>.
- [37] Cheng Yang, Maosong Sun, Wayne Xin Zhao, Zhiyuan Liu, and Edward Y. Chang. A neural network approach to jointly modeling social networks and mobile trajectories. *ACM Trans. Inf. Syst.*, 35(4):36:1–36:28, 2017. URL <https://doi.org/10.1145/3041658>.
- [38] Jie Feng, Yong Li, Chao Zhang, Funing Sun, Fanchao Meng, Ang Guo, and Depeng Jin. Deepmove: Predicting human mobility with attentional recurrent networks. In *Proceedings of the World Wide Web Conference (WWW '18)*, pages 1459–1468, 2018. URL <https://doi.org/10.1145/3178876.3186058>.
- [39] Qing Guo, Zhu Sun, Jie Zhang, and Yin-Leng Theng. An attentional recurrent neural network for personalized next location recommendation. In *Proceedings of the 34th AAAI Conference on Artificial Intelligence (AAAI '20)*, pages 83–90, 2020. URL <https://doi.org/10.1609/aaai.v34i01.5337>.
- [40] Ke Sun, Tiejun Qian, Tong Chen, Yile Liang, Quoc Viet Hung Nguyen, and Hongzhi Yin. Where to go next: Modeling long- and short-term user preferences for point-of-interest recommendation. In *Proceedings of the 34th AAAI Conference on Artificial Intelligence (AAAI '20)*, pages 214–221, 2020. URL <https://doi.org/10.1609/aaai.v34i01.5353>.
- [41] Hongyu Zang, Dongcheng Han, Xin Li, Zhifeng Wan, and Mingzhong Wang. CHA: categorical hierarchy-based attention for next POI recommendation. *ACM Trans. Inf. Syst.*, 40(1):7:1–7:22, 2022. URL <https://doi.org/10.1145/3464300>.
- [42] Yue Cui, Hao Sun, Yan Zhao, Hongzhi Yin, and Kai Zheng. Sequential-knowledge-aware next POI recommendation: A meta-learning approach. *ACM Trans. Inf. Syst.*, 40(2):23:1–23:22, 2022. URL <https://doi.org/10.1145/3460198>.
- [43] Ashish Vaswani, Noam Shazeer, Niki Parmar, Jakob Uszkoreit, Llion Jones, Aidan N Gomez, Łukasz Kaiser, and Illia Polosukhin. Attention is all you need. In *Proceedings of the Advances in Neural*

- Information Processing Systems (NeurIPS '17)*, volume 30, pages 5998–6008, 2017. URL <https://proceedings.neurips.cc/paper/2017/file/3f5ee243547dee91fbd053c1c4a845aa-Paper.pdf>.
- [44] Manzil Zaheer, Guru Guruganesh, Kumar Avinava Dubey, Joshua Ainslie, Chris Alberti, Santiago Ontañón, Philip Pham, Anirudh Ravula, Qifan Wang, Li Yang, and Amr Ahmed. Big bird: Transformers for longer sequences. In *Proceedings of the Advances in Neural Information Processing Systems (NeurIPS '20)*, 2020. URL <https://proceedings.neurips.cc/paper/2020/file/c8512d142a2d849725f31a9a7a361ab9-Paper.pdf>.
- [45] Jiezhong Qiu, Hao Ma, Omer Levy, Wen-tau Yih, Sinong Wang, and Jie Tang. Blockwise self-attention for long document understanding. In *Findings of the Association for Computational Linguistics (EMNLP '20 Findings)*, pages 2555–2565, 2020. URL <https://doi.org/10.18653/v1/2020.findings-emnlp.232>.
- [46] Yang Liu and Mirella Lapata. Hierarchical transformers for multi-document summarization. In *Proceedings of the 57th Conference of the Association for Computational Linguistics (ACL '19)*, pages 5070–5081, 2019. URL <https://doi.org/10.18653/v1/p19-1500>.
- [47] Xingxing Zhang, Furu Wei, and Ming Zhou. HIBERT: document level pre-training of hierarchical bidirectional transformers for document summarization. In *Proceedings of the 57th Conference of the Association for Computational Linguistics (ACL '19)*, pages 5059–5069, 2019. URL <https://doi.org/10.18653/v1/p19-1499>.
- [48] Liu Yang, Mingyang Zhang, Cheng Li, Michael Bendersky, and Marc Najork. Beyond 512 tokens: Siamese multi-depth transformer-based hierarchical encoder for long-form document matching. In *Proceedings of the 29th ACM International Conference on Information and Knowledge Management (CIKM '20)*, pages 1725–1734, 2020. URL <https://doi.org/10.1145/3340531.3411908>.
- [49] Chuhan Wu, Fangzhao Wu, Tao Qi, and Yongfeng Huang. Hi-transformer: Hierarchical interactive transformer for efficient and effective long document modeling. In *Proceedings of the 59th Annual Meeting of the Association for Computational Linguistics and the 11th International Joint Conference on Natural Language Processing (ACL/IJCNLP '21)*, volume 2 (Short Papers), pages 848–853, 2021. URL <https://doi.org/10.18653/v1/2021.acl-short.107>.
- [50] Alexey Dosovitskiy, Lucas Beyer, Alexander Kolesnikov, Dirk Weissenborn, Xiaohua Zhai, Thomas Unterthiner, Mostafa Dehghani, Matthias Minderer, Georg Heigold, Sylvain Gelly, Jakob Uszkoreit, and Neil Houlsby. An image is worth 16x16 words: Transformers for image recognition at scale. In *Proceeding of the 9th International Conference on Learning Representations (ICLR '21)*, 2021. URL <https://openreview.net/forum?id=YicbFdNTTy>.
- [51] Ze Liu, Yutong Lin, Yue Cao, Han Hu, Yixuan Wei, Zheng Zhang, Stephen Lin, and Baining Guo. Swin transformer: Hierarchical vision transformer using shifted windows. In *Proceeding of the IEEE/CVF International Conference on Computer Vision (ICCV '21)*, pages 9992–10002, 2021. URL <https://doi.org/10.1109/ICCV48922.2021.00986>.
- [52] Wenhai Wang, Enze Xie, Xiang Li, Deng-Ping Fan, Kaitao Song, Ding Liang, Tong Lu, Ping Luo, and Ling Shao. Pyramid vision transformer: A versatile backbone for dense prediction without convolutions. In *Proceeding of the IEEE/CVF International Conference on Computer Vision (ICCV '21)*, pages 548–558, 2021. URL <https://doi.org/10.1109/ICCV48922.2021.00061>.
- [53] Zhiyang Chen, Yousong Zhu, Chaoyang Zhao, Guosheng Hu, Wei Zeng, Jinqiao Wang, and Ming Tang. DPT: deformable patch-based transformer for visual recognition. In *Proceedings of the 29th ACM International Conference on Multimedia (MM '21)*, pages 2899–2907, 2021. URL <https://doi.org/10.1145/3474085.3475467>.
- [54] Jifeng Dai, Haozhi Qi, Yuwen Xiong, Yi Li, Guodong Zhang, Han Hu, and Yichen Wei. Deformable convolutional networks. In *Proceeding of the IEEE International Conference on Computer Vision (ICCV '17)*, pages 764–773, 2017. URL <https://doi.org/10.1109/ICCV.2017.89>.
- [55] Waldo R Tobler. A computer movie simulating urban growth in the detroit region. *Economic Geography*, 46 (sup1):234–240, 1970.
- [56] Mao Ye, Peifeng Yin, Wang-Chien Lee, and Dik Lun Lee. Exploiting geographical influence for collaborative point-of-interest recommendation. In *Proceeding of the 34th International ACM SIGIR Conference on Research and Development in Information Retrieval (SIGIR '11)*, pages 325–334, 2011. URL <https://doi.org/10.1145/2009916.2009962>.
- [57] Quan Yuan, Gao Cong, Zongyang Ma, Aixin Sun, and Nadia Magnenat-Thalmann. Time-aware point-of-interest recommendation. In *Proceeding of the 36th International ACM SIGIR Conference on Research and Development in Information Retrieval (SIGIR '13)*, pages 363–372, 2013. URL <https://doi.org/10.1145/2484028.2484030>.
- [58] Kaiming He, Xiangyu Zhang, Shaoqing Ren, and Jian Sun. Deep residual learning for image recognition. In *Proceedings of the IEEE Conference on Computer Vision and Pattern Recognition (CVPR '16)*, pages 770–778, 2016. URL <https://doi.org/10.1109/CVPR.2016.90>.
- [59] Lei Jimmy Ba, Jamie Ryan Kiros, and Geoffrey E. Hinton. Layer normalization, 2016.
- [60] Nitish Srivastava, Geoffrey E. Hinton, Alex Krizhevsky, Ilya Sutskever, and Ruslan Salakhutdinov. Dropout: A simple way to prevent neural networks from overfitting. *J. Mach. Learn. Res.*, 15(1):1929–1958, 2014. URL <https://dl.acm.org/doi/10.5555/2627435.2670313>.
- [61] Dingqi Yang, Daqing Zhang, Vincent W. Zheng, and Zhiyong Yu. Modeling user activity preference by leveraging user spatial temporal characteristics in lbsns. *IEEE Trans. Syst. Man Cybern. Syst.*, 45(1):129–142, 2015. URL <https://doi.org/10.1109/TSMC.2014.2327053>.
- [62] Dingqi Yang, Daqing Zhang, and Bingqing Qu. Participatory cultural mapping based on collective behavior

- data in location-based social networks. *ACM Trans. Intell. Syst. Technol.*, 7(3):30:1–30:23, 2016. URL <https://doi.org/10.1145/2814575>.
- [63] Xiangnan He, Lizi Liao, Hanwang Zhang, Liqiang Nie, Xia Hu, and Tat-Seng Chua. Neural collaborative filtering. In *Proceedings of the 26th International Conference on World Wide Web (WWW '17)*, pages 173–182, 2017. URL <https://doi.org/10.1145/3038912.3052569>.
 - [64] Steffen Rendle, Christoph Freudenthaler, Zeno Gantner, and Lars Schmidt-Thieme. BPR: bayesian personalized ranking from implicit feedback. In *Proceedings of the 25th Conference on Uncertainty in Artificial Intelligence (UAI '09)*, pages 452–461, 2009. URL <https://arxiv.org/abs/1205.2618>.
 - [65] Diederik P. Kingma and Jimmy Ba. Adam: A method for stochastic optimization. In *Proceedings of the 3rd International Conference on Learning Representations (ICLR '15)*, 2015. URL <http://arxiv.org/abs/1412.6980>.
 - [66] Xavier Glorot and Yoshua Bengio. Understanding the difficulty of training deep feedforward neural networks. In *Proceedings of the 13th International Conference on Artificial Intelligence and Statistics (AISTATS '10)*, volume 9, pages 249–256, 2010. URL <http://proceedings.mlr.press/v9/glorot10a.html>.